ISTANBUL TECHNICAL UNIVERSITY ★ GRADUATE SCHOOL

EFFECTIVE DOSE ESTIMATION WITH IDAC AND OLINDA PROGRAMS FOR ONCOLOGICAL PET/CT PROCEDURES

M.Sc. THESIS

Fatma Hilal BIKIRLI

Department of Nuclear Researches

Radiation Science and Technology Programme

FEBRUARY 2024

ISTANBUL TECHNICAL UNIVERSITY ★ GRADUATE SCHOOL

EFFECTIVE DOSE ESTIMATION WITH IDAC AND OLINDA PROGRAMS FOR ONCOLOGICAL PET/CT PROCEDURES

M.Sc. THESIS

Fatma Hilal BIKIRLI
(302201012)

Department of Nuclear Researches

Radiation Science and Technology Programme

Thesis Advisor: Prof. Dr. Nesrin ALTINSOY

FEBRUARY 2024

İSTANBUL TEKNİK ÜNİVERSİTESİ ★ LİSANSÜSTÜ EĞİTİM ENSTİTÜSÜ

ONKOLOJİK PET/BT TARAMALARINDA IDAC VE OLINDA PROGRAMLARI İLE ETKİN DOZ DEĞERLENDİRMESİ

YÜKSEK LİSANS TEZİ

Fatma Hilal BİKİRLİ
(302201012)

Nükleer Araştırmalar Anabilim Dalı

Radyasyon Bilim ve Teknoloji Programı

Tez Danışmanı: Prof. Dr. Nesrin ALTINSOY

ŞUBAT 2024

Fatma Hilal BIKIRLI, a M.Sc. student of ITU Graduate School student ID 302201012, successfully defended the thesis entitled “EFFECTIVE DOSE ESTIMATION WITH IDAC AND OLINDA PROGRAMS FOR ONCOLOGICAL PET/CT PROCEDURES”, which she prepared after fulfilling the requirements specified in the associated legislations, before the jury whose signatures are below.

Thesis Advisor :	**Prof. Dr. Nesrin ALTINSOY** Istanbul Technical University	.....
Jury Members :	**Prof. Dr. Ayşe Filiz BAYTAŞ** Istanbul Technical University	.....
	Assist. Prof. Dr. Türkay TOKLU Yeditepe University	.....

Date of Submission : 05 January 2024
Date of Defense : 14 February 2024

To all cancer fighters,

FOREWORD

It is with great pleasure that I present this master's thesis, the culmination of months of dedicated research and scholarly inquiry. This work represents a milestone in my academic journey and would not have been possible without the guidance and support of numerous individuals.

First and foremost, I extend my deepest gratitude to my thesis advisor, Prof. Dr. Nesrin ALTINSOY, whose expertise, insights and support have been invaluable throughout this research endeavor. Your mentorship has not only shaped the scholarly content of this thesis but has also been a source of inspiration in my academic pursuits.

I would like to express my gratitude to Assist. Prof. Dr. Turkay TOKLU for being an outstanding mentor and for your unwavering support. I am truly grateful for the opportunity to have worked with you.

Special appreciation goes to Yeditepe University Hospital Nuclear Medicine Department for providing the necessary resources, including access to patient databases, and laboratories, fostering an environment conducive to rigorous academic exploration.

Finally, to all those who may find themselves perusing the pages of this thesis, I hope that the insights garnered from this research contribute meaningfully to the existing body of knowledge in medical radiation. It is my sincere hope that this work stimulates further discussion, inquiry, and exploration in the realms of Dose Assessment in Nuclear Medicine.

Thank you to everyone who has played a role in the realization of this academic endeavor.

January 2024

Fatma Hilal BIKIRLI
(Biomedical Engineer)

TABLE OF CONTENTS

Page

ABBREVIATIONS

CF	**:** Conversion Factor
CT	**:** Computed Tomography
CTDI	**:** Computed Tomography Dose Index
DLP	**:** Dose Length Product
ED	**:** Effective Dose
FDG	**:** Florodeoksiglukoz
IAEA	**:** International Atomic Energy Agency
ICRP	**:** International Commission on Radiological Protection
ImPACT	**:** Imaging Performance Assessment of CT Scanners
MeV	**:** Mega-electronvolt (unit of energy)
MIRD	**:** Medical Internal Radiation Dose
MRI	**:** Magnetic Resonance Imaging
OLINDA/EXM	**:** Organ Level INternal Dose Assessment for Exponential Modeling
DCAL	**:** Dose and Risk Calculation
PACS	**:** Picture Archiving and Communication System
PET	**:** Positron Emission Tomography
PSMA	**:** Prostate-Specific Membrane Antigen
RADAR	**:** Radiation Dose Assessment Resource
ROI	**:** Region of Interest
SNMMI	**:** Society of Nuclear Medicine and Molecular Imaging
SPECT	**:** Single-Photon Emission Computed Tomography
S-values	**:** Specific Absorbed Fractions

SYMBOLS

Gy	**:** Gray (unit of absorbed dose)
mGy	**:** Milligray
mSv	**:** Millisievert (unit of effective dose)
kVp	**:** Kilovolt Peak
mA	**:** Milliampere
Bq	**:** Becquerel (unit of radioactivity)
Ci	**:** Curie (unit of radioactivity)
w_T	**:** Tissue Weighting Factor
A_s	**:** Accumulated source activity at time (t)
A_0	**:** Administered activity
F_s	**:** Fraction of pharmaceutical which is the fraction of radiation accumulated in the organ
λ_e	**:** Effective decay constant
SD	**:** Standard Deviation

LIST OF TABLES

Page

LIST OF FIGURES

Page

EFFECTIVE DOSE ESTIMATION WITH IDAC AND OLINDA PROGRAMS FOR ONCOLOGICAL PET/CT PROCEDURES

SUMMARY

PET/CT imaging, which combines Positron Emission Tomography (PET) with Computed Tomography (CT), exposes human bodies to high radiation doses. This is because of the radiation emitted by positron-emitting substances and the X-rays used in the procedure. This retrospective study is carried out to provide an insight into the effective dose value on patients in oncological procedures.

In this study, PET/CT studies of 305 patients in Yeditepe University Kosuyolu Hospital performed on January 2023 were reviewed for radiopharmaceutical ^{18}F-FDG and ^{68}Ga-PSMA. 220 patients were performed with ^{18}F-FDG and rest of 85 patients was with ^{68}Ga-PSMA. Data analysis of each patient is classified as weight, height, gender, volume Computed Tomography Dose Index ($CTDI_{vol}$), Dose Length Product (DLP) and radiopharmaceutical administered. IDAC and OLINDA softwares were chosen among various methods of calculating effective dose values for PET/CT exam. These programs are widely used for diagnostic nuclear medicine based on the International Commission on Radiological Protection (ICRP) regulations of 1991 and 2007 tagged ICRP 60 and ICRP 103 respectively.

Biokinetic data for ^{18}F and ^{68}Ga radionuclides are registered into IDAC and OLINDA programs to estimate the effective dose for the oncology patients. Effective dose from the CT scan was calculated via ImPACT software program. Adding this to the effective dose from the PET scan gave us the total effective dose for the combined PET/CT procedures.

OLINDA software calculates the effective dose only with ICRP 60 tissue weighting factors whereas IDAC softwares estimate effective dose based on both ICRP 60 and ICRP 103 tissue weigting factors. Also, IDAC software employs both old and new phantom as presented in ICRP 23 and ICRP 110, respectively. OLINDA software only employ the mathematical phantom presented in ICRP 23.Whole body ^{18}F-FDG PET/CT total effective dose values obtained by IDAC (new phantom) and OLINDA programs based on ICRP 60 were calculated as 26.1±3.5 mSv and 29.0±3.7 mSv, respectively. ^{18}Ga-PSMA PET/CT effective doses obtained by IDAC (new phantom) and OLINDA were 22.2±3.1 mSv and 23.8±3.2 mSv, respectively. The PET doses from highest to lowest were calculated with OLINDA (old phantom, ICRP 60), IDAC (old phantom, ICRP 60), IDAC (new phantom, ICRP 60) and IDAC (new phantom, ICRP 103) as 9.36, 9.07, 7.01, 6.28 mSv respectively for ^{18}F-FDG. The highest PET effective dose was also calculated with OLINDA software as 3.65 mSv for ^{68}Ga-PSMA. In whole body protocols, the highest contribution to the total effective dose comes from CT scans. For ^{68}Ga-PSMA protocols, CT contribution to the total effective dose is ~92%. For ^{18}F-FDG protocols, the contribution of CT effective dose to the total effective dose was ~75%.

ONKOLOJİK PET/BT TARAMALARINDA IDAC VE OLINDA PROGRAMLARI İLE ETKİN DOZ DEĞERLENDİRMESİ

ÖZET

Günümüzde nükleer tıpta birçok görüntüleme tekniği kullanılmaktadır. Görüntüleme tekniklerinde, detaylı görüntünün, sağlıklı dokuya minimum radyasyon hasarı ile alınması hedeflenmektedir. Son geliştirilen tekniklerden PET (Pozitron Emisyon Tomografisi) görüntüleme yöntemi ile herhangi bir organın çalışmasındaki bozukluk hücre düzeyinde tespit edilebilmektedir. Vücutta gözle görülebilir değişikliklerden önce metabolik değişiklikler meydana gelmektedir. PET taramalarında metabolik değişiklikler tespit edilebildiği için lezyon hakkında, diğer yöntemlere nazaran daha erken bilgi elde edilebilmektedir.

PET görüntüleme, anhilasyon fotonlarının deteksiyonuna dayanan bir yöntemdir. Bu yöntemde, vücuda pozitron yayan radyofarmasötikler verilmektedir. ^{18}F ve ^{68}Ga yaygın kullanımı olan PET radyonüklitleri olup parçalandıkları zaman pozitron salınımı yaparlar. PET çalışmaları ile moleküler düzeyde duyarlılığın artmasını sağlayan fonksiyonel görüntüler elde edilir. Ancak, yapısal görüntüleme yeteneği yoktur. 1998 yılında PET sistemleri Bilgisayarlı Tomografi (BT) ile birleştirilerek PET/BT sistemi geliştirilmiştir. Böylece PET fonksiyonel bilgileri ile eş zamanlı olarak anatomik bilgilerin elde edilmesi sağlanmıştır.

PET/BT görüntüleme tekniği onkoloji, kardiyoloji ve nörolojide yaygın olarak kullanılmaktadır. Onkolojide kullanımı, kanser tanısının yanı sıra evrelendirme ve tedaviye yanıtın değerlendirilmesini içermektedir. PET/BT taramalarında radyofarmasötiklerin ve X-ışınının bir arada kullanımına bağlı olarak radyasyon maruziyetindeki artış nedeniyle hasta dozu da artmaktadır. Radyasyonun hasta üzerindeki etkilerini değerlendirerek, radyasyon maruziyetini kontrol altında tutmak ve asgariye indirmek önemlidir.

Doku veya organların aldığı dozun tüm vücutta oluşturduğu riski ifade etmek için etkin doz kavramı kullanılmaktadır. Organ ve dokuların maruz kaldığı radyasyonun cinsine ve miktarına bağlı olarak farklılık gösteren bu değer, radyasyonun genel etkilerini birleştirerek vücut üzerindeki toplam radyasyon etkisini temsil eder. Etkin doz, ICRP (Uluslararası Radyasyondan Korunma Komisyonu) tarafından belirlenen bir kavramdır ve radyasyonun biyolojik etkilerini değerlendirmek amacıyla kullanılır. ICRP, radyasyon dozlarını değerlendirmek ve standartlaştırmak amacıyla farklı radyasyon türleri ve dokular için ağırlık faktörlerini belirlemiştir. ICRP 60 ve ICRP 103 yayınları ağırlık faktörleriyle ilgili detaylı bilgileri içermektedir. Etkin doz, organ ve dokuların maruz kaldığı radyasyonun türü ve miktarına bağlı olarak ICRP tarafından önerilen ağırlık faktörleri kullanılarak hesaplanmaktadır.

OLINDA (Organ Level Internal Dose Assessment) ve IDAC (Internal Dose Assessment by Computer) yazılımları, nükleer tıpta kullanılan, radyasyon dozu hesaplamaları için geliştirilmiş programlardır. Her iki program da radyasyon doz

hesaplamalarında ICRP modellerini ve veritabanlarını kullanmaktadır. Söz konusu yazılımlar nükleer tıpta radyasyon doz tahminleri yapma konusunda uzmanlaşmış olup klinik uygulamalarda önemli rol oynamaktadırlar. Ancak, kullanım alanları ve detayları spesifik uygulamalara göre değişebilmektedir.

ImPACT (Imaging Performance Assessment of CT Scanners) BT doz hesaplama programı, bilgisayarlı tomografi (BT) cihazlarının radyasyon dozlarını değerlendirmek için kullanılan bir yazılımdır. Bu program, BT taramalarının radyasyon dozlarını tahmin etmek ve optimize etmek amacıyla tasarlanmıştır. ImPACT, matematiksel modeller kullanarak tüp akımı ve gerilimine bağlı olarak radyasyon dozunu tahmin eder. ImPACT, ICRP ve diğer ilgili kuruluşların standartlarına uygun olarak tasarlanmıştır.

Güncellenen ICRP yayınları ile birlikte doku ağırlık faktörleri de güncellenmektedir ve buna bağlı olarak aynı tıbbi prosedür için elde edilen etkin doz değerleri de değişmektedir. Değişen doku ağırlık faktörlerinin yanı sıra yazılım programlarında farklı fantomların kullanılması da etkin dozu etkilemektedir. Tüm bu değişkenler aynı PET/BT prosedürü için farklı etkin doz değerlerinin hesaplanmasına neden olmaktadır.

Bu retrospektif çalışma, onkolojik prosedürlerde hastaların üzerindeki etkin doz değerlerine ilişkin bir irdeleme yapmak amacıyla gerçekleştirilmiştir. Bu çalışmada, günümüzde yaygın uygulaması olan PET/BT prosedürleri ele alınmış ve kullanılan radyofarmasötiklere ilişkin olarak hastanın farklı organ ve dokuları için radyasyon dozları hesaplanmıştır. Bu hesaplamalar, ICRP standartlarına ve modellerine uygun olarak yapılmıştır. Organ ve dokulardaki radyasyonun etkilerinden yola çıkarak tüm vücut dozunu değerlendirebilmek için etkin doz hesaplanmıştır.

Yeditepe Üniversitesi Koşuyolu Hastanesi'nde Ocak 2023 de gerçekleştirilen çalışmada 305 hastanın ^{18}F-FDG ve ^{68}Ga-PSMA radyofarmasötikleri ile yapılan PET/BT taramalarına ilişkin kayıtlar incelenmiştir. 220 hasta ^{18}F-FDG ve kalan 85 hasta ^{68}Ga-PSMA protokolü uygulanan hastalardır. Hastalar ağırlık, boy, cinsiyet, Bilgisayarlı Tomografi Doz İndeksi ($CTDI_{vol}$), Doz Uzunluk Çarpımı (DLP) ve uygulanan radyofarmasötik açısından sınıflandırıldıktan sonra OLINDA, IDAC ve ImPACT programları kullanılarak etkin dozlar elde edilmiştir. Her iki radyofarmasötik için yazılım programları ile elde edilen sonuçlar irdelenmiştir.

Toplam 305 hasta kaydının incelendiği çalışmada etkin dozlar ICRP 60 ve ICRP 103 organ ağırlık faktörleri kullanılarak tespit edilmiştir. IDAC ile ICRP 103'ün organ ağırlık faktörleri dikkate alındığında tüm vücut ^{18}F-FDG ve ^{68}Ga-PSMA protokolleri için PET/BT ortalama etkin doz değerleri sırasıyla 25.3±3.2 mSv ve 22.0±3.1 mSv olarak elde edilmiştir. IDAC, ICRP 60'ın organ ağırlık faktörleri dikkate alındığında ise tüm vücut ^{18}F-FDG ve ^{68}Ga-PSMA protokolleri için PET/BT ortalama etkin doz sırasıyla 26.1±3.5 mSv ve 22.2±3.1 mSv olarak hesaplanmıştır.

OLINDA programı sadece ICRP 60'ın organ ağırlık faktörü ile etkin doz hesabı yapmaktadır. Tüm vücut ^{18}F-FDG ve ^{68}Ga-PSMA etkin doz ortalamaları sırasıyla 29.0±3.7 mSv ve 23.8±3.2 mSv olarak hesaplanmıştır. IDAC ve OLINDA programları ile ICRP 60'da yer alan organ ağırlık faktörleri kullanılarak elde edilen etkin doz değerleri değişkenlik göstermektedir. Bunun nedeni, programlarda farklı matematiksel modellerin ve farklı fantomların kullanılıyor olmasıdır. OLINDA yazılımı, ICRP 23 kılavuzunda açıklanan matematiksel fantom ile doz hesaplamasını gerçekleştirmektedir. IDAC yazılımı, ICRP 110 kılavuzunda yayınlanan güncel

fantomları kullanmaktadır. IDAC Yazılımı aynı zamanda, ICRP 23 kılavuzda açıklanan eski fantomu temel alarak da efektif doz hesaplaması yapmaktadır.

^{18}F-FDG PET etkin doz değerleri en yüksekten en düşüğe doğru OLINDA (eski fantom, ICRP 60), IDAC (eski fantom, ICRP 60), IDAC (yeni fantom, ICRP 60) ve IDAC (yeni fantom, ICRP 103) ile sırasıyla 9.36, 9.07, 7.01, 6.28 mSv olarak hesaplanmıştır. ^{68}Ga-PSMA protokolleri için IDAC programında ICRP 110'da yer alan fantoma dayalı hesaplamalarda, ICRP 60 ve 103 kılavuzlarında yer alan her iki organ ağırlık faktörleri için elde edilen etkin doz değerleri sırasıyla, 2.07 mSv and 1.83 mSv olarak hesaplanmıştır. ^{68}Ga-PSMA için en yüksek PET etkin doz değeri OLINDA yazılımı ile 3.65 mSv olarak elde edilmiştir.

Her iki protokol için ulaşılan sonuçlar bir arada değerlendirildiğinde ICRP 103 doku ağırlık faktörlerini içeren güncel IDAC yazılımının IDAC'ın eski versiyonuna ve OLINDA yazılımına göre daha düşük PET etkin doz değerleri hesapladığı sonucuna varılmıştır.

Tüm vücut protokollerinde toplam etkin doza en büyük katkı BT çekimlerinden gelmektedir. ^{68}Ga-PSMA protokolleri için toplam etkin doza BT katkısı ~%92 dir. ^{18}F-FDG protokolleri için BT etkin dozunun toplam etkin doza katkısı ~%75 olmuştur.

Çalışmada hesaplanan dozlar genel bir referans bireye ilişkindir. Her hastanın aldığı PET dozlarının daha gerçekçi bir analizi için bireysel biyokinetik, anatomik ve fizyolojik özellikler hakkında ek bilgilere ihtiyaç vardır.

1. INTRODUCTION

Around all of us, there is always a source of radiation. They vary between natural sources and the ones that are produced by artificial sources. X-ray machines and radiopharmaceuticals which are used in diagnostics or radiotherapy and other various medical devices makes the most of artificial sources of exposure to radiation for humans (WHO, 2023).

It has been more than a century since ionizing radiation started to be used in diagnostics (Amis et al., 2007). Since the 1950's, there has been several advancements for the developing of nuclear medicine imaging modalities and radiopharmaceuticals. Many improvements have been made during 1980's starting from the use of rectilinear scanners, gamma cameras that are able to perform dynamic studies and SPECT with a single and multi-detected gamma cameras. During the 2000s, PET and SPECT have begun to be unified with CT as PET/CT and SPECT/CT. In 1998 the first combination of PET was with CT was made, after that it started to be used regularly all over the world in 2001.

Naturally this significant improvement and spreading of imaging also caused a large increase in the exposure of the world population to the ionizing radiation (Amis et al., 2007). The dramatic increase in the usage of computed tomography (CT), interventional radiology and nuclear medicine is the biggest reason behind this increased exposure that is sourced by medical imaging (NCRP, 2009). Just like all around the World, the use of PET during the development and formulation of novel PET radiopharmaceuticals is also becoming increasingly popular in Turkey (Günay and Özer, 2016). In order to get the special benefits of both positron emission tomography and computed tomography (PET/CT), imaging with an equipment that combines both of them during one procedure is required. This imaging technique which is very sensitive is used in oncology, cardiology, neurology as well as in infectious and inflammatory diseases.

Even though the information that's gotten from the PET scan and CT scan is different they do complete each other. The difference is that the PET scan shows the body parts

with increased levels of metabolic activity but the CT scan shows a more detailed anatomical location. However, an increased amount of radiation exposure in patients was detected during PET/CT examinations compared to an individual scan with PET or CT, this is a result of combining of the doses from both PET and CT (Huang, 2009).

Mostly as a radiotracer PET uses ^{18}F-FDG, the reason is that it has a relatively shorter half-life (110 min) which helps to reduce the exposure to radiation when compared to the other widely utilized radionuclides like 99mTechnetium (6 hours) and 201Thallium (72 hours). When the radiation exposure is from 18F it causes to the patient an internal exposure while a low level of external exposure to the people nearby. The radiation (X-rays) that is sourced from a CT scanner will only radiate the patient and it's only during the scanning process (URL-10).

^{68}Ga-PSMA is another widely utilized radiotracer in PET. PSMA which stands for "prostate-specific membrane antigen" is a type of protein that can be found on the surface of prostate cancer cells. Ga-68 PSMA PET/CT is a kind of medical imaging which utilizes a Ga-68 tracer that is labeled with a molecule which binds to PSMA. This enables the tracer to assemble in the prostate cancer cells, after that it will be detected by a PET/CT scanner.

It is crucial to gather data on the administrated activity of PET tracer and DLP and CTDIvol parameters of CT scan in order to estimate the patient dose in PET/CT. While evaluating relative biologic risk, the effective dose is widely utilized and it can be calculated by using above parameters. The ICRP defines it as the tissue-weighted sum of the equivalent doses within all of the specified tissues and organs of the body of a human and shows the stochastic health risk to the whole body (Climent et al., 2017). In order to represent the entire body burden, the effective doses from PET and CT are calculated and combined (Quinn et al., 2016).

1.1 Literature Review

Various software programs employed for dose estimation in the literature were investigated. The obtained results from diverse phantoms and biokinetic data sets were analyzed and compared. The impact of incorporating updated mathematical models and biokinetic data on the calculation of effective dose was assessed.

Climent et al. (2017) retrospectively analyzed the PET/CT procedures involving various radiopharmaceuticals for 210 patients. They evaluated effective dose for the patients undergone the procedures across different protocols, such as Brain, Whole Body, Torso, Head and Neck Tumor. The study covered radiopharmaceuticals like ^{18}F-florbetapir, ^{18}FDG, ^{11}C-MET, ^{11}C-CHOL and ^{18}FDOPA. By applying conversion factors to the radiopharmaceutical activity and CT-DLP, they found that the mean effective dose for whole body and brain PET/CT procedures varying from 4.6 to 20.0 mSv. CT scans significantly contributed to total ED for whole body studies, while PET radiopharmaceuticals are the major contributor in brain studies.

Quinn et al. (2016) conducted a review of whole-body PET/CT exams, comparing two patient groups one with a standard CT and the other with a diagnostic CT. They used patient specific data to calculate the radiation doses coming from PET and CT imaging. The mean effective dose for patients who received ^{18}F-FDG was 9.0±1.6 mSv. The mean of total effective dose in standard PET/CT was 14±1.3 mSv, and in diagnostic PET/CT, it was 24.4±4.3 mSv. The study found that the bladder, brain, heart, lungs, and liver consistently received the highest equivalent doses in all examinations.

Akpochafor et al. (2018) used the imPACT software to estimate mean organ doses from seven randomly selected CT units (A-G). They employed the imPACT Patient Dosimetry Calculator to determine organ doses for the head, chest, abdomen, and pelvic region based on CT parameters from 210 patients. The data analysis, conducted using SPSS 16.0, revealed statistically significant differences in organ doses for the brain, eye lens, lungs, breast, thyroid, heart, stomach, liver, bladder, and uterus among the seven CT units.

Ekpo et al. (2018) examined data from 171 patients to assess the CT-Expo software's ability to determine key parameters like CTDIvol, DLP, effective dose and organ dose. The study included patient data from a Toshiba Aquillion 16-slice CT scanner (CT unit A) and a Philips Brilliance 16-slice CT scanner (CT unit B). The CT-Expo software, which was used for dose estimation, demonstrated good agreement with the imPACT software program from the ImPACT scanner assessment group in London, UK. Notably, CT unit A exhibited more significant discrepancies in DLP and CTDIvol compared to unit B, possibly due to variations in the kVp and pitch settings of the scanners.

Abuqbeitah et al. (2022) examined the cumulative effective dose (CED), frequency and clinical reasons for the patients going through multiple ^{18}F-FDG PET/CT scans. They conducted a retrospective analysis of 55.424 scans over 11 years at a university hospital. The effective dose was calculated based on administered activity and DLP. The study revealed a substantial number of patients, mainly with malignancies (82%), go through repeated imaging within a year, with a notable portion exceeding 100 mSv in a year. This extensive 11-year analysis provides valuable insights into the patterns and radiation exposure of patients in recurrent ^{18}F-FDG PET/CT procedures.

Demirci et al. (2018) examined the absorbed doses of ^{68}Ga-PSMA -11, focusing on seven patients with a mean age of 66.9±6.6 years. They utilized whole-body PET imaging at various time spots and used the OLINDA/EXM, MIRD method and NUKFIT software programs for internal dosimetry estimations. The kidneys, salivary, bladder wall and lacrimal glands received the highest absorbed doses with estimated doses after a 150 MBq injection of ^{68}Ga-PSMA-11 being 37.0, 12.6, 14.4, and 6.3 mSv, respectively. The effective dose from PET imaging with 150 MBq injected ^{68}Ga-PSMA-11 was 2.5 mSv. In summary, ^{68}Ga-PSMA-11 exhibited a suitable dosimetry profile similar to clinically used ^{68}Ga-labeled octreotide analogs, which have a longstanding record of safe use in routine clinical studies. Any adverse effects were not observed, and the kidneys were identified as the organs with the dose limitations.

Kamp et al. (2023) carried out a review of existing biokinetic data, gathered new experimental data, and introduced an updated compartmental model for 2-[18F] FDG as part of the ICRP publication 128 revision. The model, developed using published data and additional information from 23 patients undergoing PET/CT, was refined with SAAM II software and validated using a updated model of IDAC-Iodide. Dose coefficients for standard reference man were computed using IDAC-Dose 2.1, incorporating a dynamic bladder model for urinary bladder dosimetry. The recommended model includes sections for kidneys, heart wall, blood, brain, liver, pancreas, lungs, urinary bladder content, spleen and a generic pool section labeled "Other''. The effective dose coefficient, in line with the contemporary ICRP dosimetry framework, was 1.7E-02 mSv/MBq, compared to 1.9E-02 mSv/MBq as indicated in ICRP Publication 128.

Karim et al. (2023) evaluated the internal dosimetry for patients who underwent a PET imaging with the ^{18}F-FDG radiopharmaceutical. They studied 24 patients diagnosed

with lymphoma, administering an average of 300.80±23.09 MBq of ^{18}F-FDG for a whole-body PET imaging. The IDAC-Dose 2.1 software program from the ICRP measured effective and absorbed doses. Organs analyzed for absorbed dose included as followed the brain, liver, adrenals, kidneys and breast. The brain showed the highest absorbed dose, while the breast showed the lowest. Total effective dose for all patients was 4.85±0.37 mSv, and the effective dose to administered activity ratio was 1.611×10^{-2} mSv/MBq. The study affirmed the safety of actual ^{18}F-FDG PET scan practices, as the effective dose to injected activity ratio was below the threshold of $1.9x10^{-2}$ mSv/MBq.

Lacerda et al. (2019) aimed to evaluate the dosimetric accuracy of OLINDA/EXM software program and ICRP publication 106 against an patient-specific dosimetric approach. Various methods exist for estimating absorbed doses from internal radionuclides, differing in the anatomical phantom models used for internal dosimetric calculations. ICRP 89 include the phantoms based on medical imaging data from the mean population in Eastern Europe and North America, as OLINDA/EXM uses stylized anatomical models from the 1960s, modeled after the 'Reference Man' described by ICRP 23. Comparing these methods performed relative error which is a measure quantifying the inconsistency between two sets of data. Relative errors were computed for conversion coefficients in lungs, liver, cortical bone, skin, brain and kidney. It is resulted that the lungs, brain and liver showed the lowest relative error values since these organs have a higher uptake of the ^{18}F-FDG and are identified as source organs according to the ICRP in this specific biokinetic model.

1.2 Purpose of Thesis

The purpose of this study was to retrospectively examine the effective dose for the patients going through PET/CT scans by using computational tools. This study focuses on two radiopharmaceuticals, ^{18}F-FDG and ^{68}Ga-PSMA, given to patients for a cancer imaging study. This retrospective study was performed on 305 patients at nuclear medicine department in Yeditepe University Koşuyolu Hospital by classifying the data $CTDI_{vol}$ (mGy) and DLP (mGycm). The patients' internal dosimetry will be calculated with IDAC and OLINDA methodologies to identify effective dose deposited in patients according to ICRP 60 and 103. Due to anatomical and malignant

variance between patients, specific effective dose was administered to each patient and these values changed based on weighting factors published by ICRP.

The research delves into the methodology and algorithms employed by IDAC and OLINDA software programs, critically evaluating their capabilities in predicting absorbed doses to specific organs and tissues. Both software programs employ biokinetic models, compartmental modeling, and other mathematical frameworks to simulate the complex interplay of radionuclide distribution, biological kinetics, and radiation interactions within the human body.

The findings of this research contribute to the ongoing refinement and improvement of effective dose assessment methodologies in nuclear medicine. By enhancing our understanding of the strengths and limitations of IDAC and OLINDA, this study aims to provide valuable insights for healthcare professionals, physicists, and researchers involved in nuclear medicine practices, ultimately contributing to the advancement of patient care and radiation safety in the medical field.

1.3 Hypothesis

The utilization of IDAC and OLINDA software programs for effective dose assessment in nuclear medicine applications will demonstrate comparable accuracy in predicting absorbed doses to specific organs and tissues. The hypothesis posits that the two software tools, despite differences in their modeling approaches, will yield consistent results with the literature across a range of radiopharmaceuticals and patient scenarios. The study anticipates that advancements in computational modeling, coupled with the evolving understanding of biokinetics and radiation interactions, will contribute to the robustness of both IDAC and OLINDA in predicting effective doses. Through comprehensive analyses, this research aims to providing valuable insights into the reliability and applicability of these tools for optimizing radiation safety in nuclear medicine procedures.

2. THEORY

Radioactive materials emit energy in the form of radiation, which can be waves or particles. Ionizing radiation, including common forms like X-rays and gamma rays, is used daily in medical procedures for diagnostic imaging and interventions. Interactions of ionizing radiations with matter are fundamental to the practice of radiation protection. They determine the magnitude and distribution of doses in tissues, the performance of detectors and imaging devices, and the attenuating properties of shielding materials.

2.1 Interaction of Electromagnetic Radiation with Matter

The principle mechanisms of energy deposition by photons in matter are photoelectric absorption, Compton scattering and pair production (Turner, 2007).

2.1.1 Photoelectric effect

When a photon interacts with an atom, it can transfer its entire energy to an electron. This transaction results in the release of atoms and electrons, forming ion pairs. The energy of the emitted electron (photoelectron) is determined by subtracting the binding energy of the electron from the energy of the incident photon. The energy of photoelectron (E) is given by

$$E = E\gamma - \varphi \tag{2.1}$$

Here E_γ is the energy of the incoming photon and φ is the binding energy for electrons in the atomic shell (Stabin, 2007). This binding energy is the nessesary limit to release the electron from the atom. The ejected electrons behave like beta particles, causing ionization (secondary ionization) as they move inside matter.

Figure 2.1 illustrates photoelectric effect as below and when an electron is extracted from the inner shell of an atom, the outer shell electron descends from a higher energy state to occupy the empty position. This energy shift in states require the release of energy from the atom, which appear as soft (low-energy) X-rays. X-rays have the same

properties as gamma rays. The main difference derives from their origins. Gamma rays result from energy state shifts in atomic nuclei, and X-ray result from energy state shifts in atomic electrons (Attix, 1986).

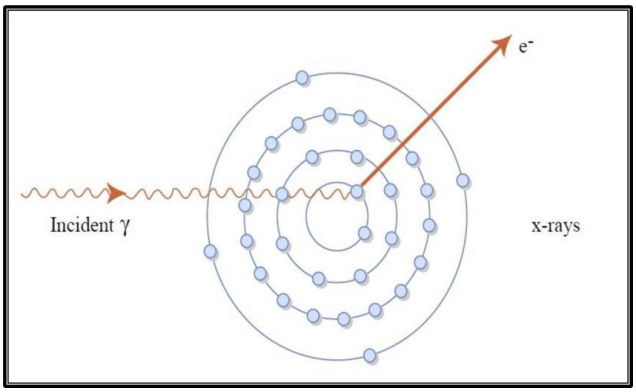

Figure 2.1 : Photoelectric Effect (URL-1).

2.1.2 Compton effect

When photons, like X-rays and gamma rays, interact with atoms, they can share some of their energy with electrons in a process called the Compton effect or Compton scattering. The photon is as a little energy package that bumps into an electron. Instead of giving all its energy to the electron, the photon shares only a part of it. This causes the electron to move at a different angle than the original path of the photon. This interaction called the Compton effect.

As a result of Compton scattering, ion pairs are created, similar to photoelectric effect. Other than that, there is an interesting twist: the photon, after being deflected, can interact with other electrons in a similar way, or it can go through other interaction processes as it travels through matter. The photon keeps moving until it loses all its kinetic energy. The electrons that get released during this process behave like beta particles, and they lose their energy by causing more ionization of other electrons, like a chain reaction. So, in simple terms, when photons interact with atoms, they can share their energy with electrons, leading to the creation of ion pairs and a gradual of events that involve the movement of electrons and the release of energy (Attix, 1986).

Figure 2.2 illustrate the compton scattering and the wavelenght is calculated as below;

$$\Delta\lambda = \lambda' - \lambda = \lambda_c(1-\cos\theta) \tag{2.2}$$

In the equation above;

λ: wavelength for the incoming photon

λ' : wavelength for the scattered photon

λ_c : Compton wavelength of the electron

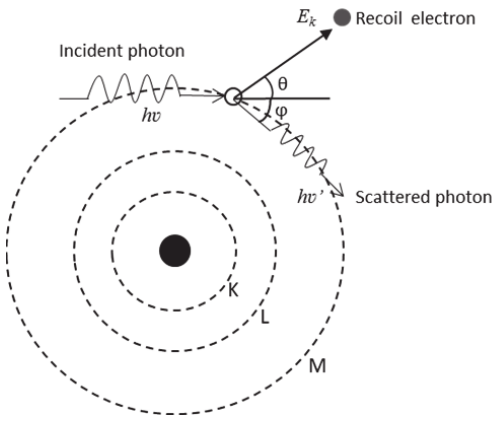

Figure 2.2 : Compton Scattering (URL-2).

2.1.3 Pair Production

The interactions of gamma rays and matter that have been considered so far involve the transfer of all or part of the energy to the electrons of the irradiated matter. Another mechanism as pair production, leads to the form of nuclear particles from energy. The nuclear particles generated are negatrons and positrons from single gamma-ray photons interacting with the Coulomb field of the nucleus (Attix, 1986).

This phenomenon has been illustrated in Figure 2.3 and this interaction leads to the production of mass from energy. The production of an electron necessitate a specific quantum of energy from a gamma-ray photon. This energy (E) is found out applying Einstein's equation as shown below;

$$E = m \times c^2 \tag{2.3}$$

In the equation, m is mass and c is speed of light.

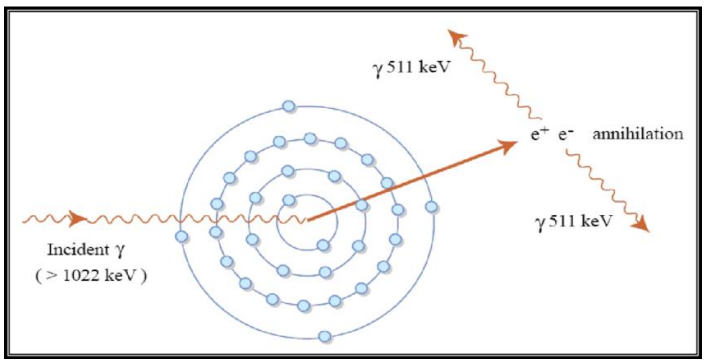

Figure 2.3 : Pair Production (URL-3).

2.2 Internal Dosimetry

Internal radiation dosimetry is described as the quantitative assessment and calculation of the radiation dose delivered to specific organs and tissues within the patient body due to radioactive substances, known as radionuclides. This process is a crucial aspect of nuclear medicine and radiation protection, as it helps quantify the amount of radiation absorbed by various organs during medical procedures involving the administration of radioactive materials.

Internal radiation dosimetry is particularly relevant when patients are administered radiopharmaceuticals for diagnostic imaging or therapeutic purposes. Radiopharmaceuticals contain radioactive isotopes that emit radiation. After administration, the radiopharmaceutical undergoes biodistribution, where it is distributed throughout the body. Biokinetic studies the movement and elimination of the radioactive matter within the body over time.

The process involves the use of sophisticated computational models that simulate the behavior of the radioactive material within the body. These models consider factors such as organ sizes, shapes, and anatomical variations. Various dosimetry tools and software programs are used to perform internal radiation dosimetry calculations. These tools utilize mathematical models, data from biokinetic studies, and anatomical information to estimate the radiation dose received by specific organs and tissues. The term of effective dose is often used in internal radiation dosimetry. Internal radiation dosimetry aims to provide patient-specific information. It considers factors such as the patient's age, gender, weight, and specific characteristics of the administered radiopharmaceutical. In diagnostic nuclear medicine, internal radiation dosimetry is crucial for optimizing imaging protocols and ensuring patient safety. In therapeutic nuclear medicine, it plays a key role in treatment planning, monitoring, and adjusting therapeutic doses to achieve desired clinical outcomes. Internal radiation dosimetry is fundamental to provide that radiation exposure within ALARA limits while ascertaining clinically helpful information.

Accurate internal radiation dosimetry is essential for balancing the benefits of nuclear medicine procedures with potential risks, ensuring patient safety, and contributing to the advancement of personalized medicine in the context of radiological practices (Powsner et al., 2013).

2.2.1 Absorbed dose

The primary physical quantity used in dosimetry is the absorbed dose. Absorbed dose is a measure of the amount of energy absorbed by a substance or material per unit mass. It quantifies the energy given to a matter by ionizing radiation. This term in medical contexts is particularly important as absorbed dose is used to determine the amount of radiation energy delivered to a specific tissue or organ during oncological procedures (Powsner et al., 2013). The unit of absorbed dose is J/kg (Gy). The traditional unit, the rad, is defined as 100 erg/gr. The absorbed dose is often referred to simply as the dose.

2.2.2 Equivalent dose

Equivalent dose is defined for any kind of radiation, but only in human tissue. It is a measure adapted for specific organs and is based on the absorbed dose to account for the effectiveness of the radiation type on that individual organ. In essence, this term allows to have insight for a more specific evaluation of the biological impact of radiation on different body parts (Powsner et al., 2013). The International Commission on Radiological Protection (ICRP), National Council on Radiation Protection and Measurements (NCRP) as well as International Commission on Radiation Units (ICRU) have introduced a new concept of the dose equivalent for radiation protection purposes in order for the different biological effectiveness of different kinds of radiation to be allowed. The dose equivalent (H_T) is defined as the product of the absorbed dose (D) and quality factor (Q) which depends on Linear Energy Transfer (LET). Quality factor is dimensionless, so the the units are the same as absorbed dose. Special unit of the equivalent dose is sievert (Sv). The traditional unit of equivalent dose was rem and 1 rem = 0.01 J/kg = 0.01 Sv.

The ICRP and NCRP replaced the quality factors by radiation weighting factors (w) by the early 1990s (Turner, 2007). The radiation weighting factor is one for gamma and beta radiations.

Table 2.1 : Radiation Weighting Factors (ICRP 103, 2007).

Radiation type	Radiation weighting factor, w_R
Photons	1
Electrons and muons	1
Protons and charged pions	2
Alpha Particles, fission fragments, heavy Ions	20
Neutrons	A continuous function of neutron energy

2.2.3 Effective dose

Since different tissues of the body respond differently to radiation, the probability for stochastic effects that result from a given equivalent dose will generally depend upon the particular tissue or organ irradiated. To take such differences into account, the ICRP and NCRP have assigned dimensionless tissue weighting factors (Turner, 2007).

Effective dose accounts for external and internal radiation exposures, providing a total assessment of the potential biological effects on a reference person. ICRPs provide precise, age- and sex-averaged tissue weighting factors as specific normalized values. These factors describe how different tissues contribute to the radiation damage caused by stochastic effects from low energy transfer throughout the whole body. The term of effective dose, a single dosimetric measure tied to risk, serves both prospective planning and retrospective assessments to ensure compliance with dose limits and restrictions (Powsner et al., 2013). Effective dose (ED) is calculated as below;

$$ED = \sum(w_T \times H_T) \tag{2.4}$$

Here, w_T is tissue weighting factor and H_T is the equivalent dose. Effective dose is expressed in sievert (Sv*)*, or, more frequently, millisievert (mSv) which is 1/1000th of a sievert.

2.3 The History of Radiation Use in Medicine

The history of radiation use in medicine is a fascinating journey marked by significant discoveries, breakthroughs, and advancements. In 1895, Wilhelm Conrad Roentgen by accident discovered X-rays, while performing the experiment with cathode rays. This

discovery revolutionized medicine by providing a new means of visualizing the internal structures of the human body without invasive procedures.

Radiography quickly became a standard diagnostic tool in medicine. X-rays were used for imaging bones, detecting fractures, and visualizing internal organs in 1896-1900. Figure 2.4 shows the first picture of medical X-ray by Anna Bertha Ludwig's hand who is Wilhem Roenthen's wife in 1896. By the early 20th century, X-ray technology had become widespread in medical practice.

Figure 2.4 : Anna Bertha Ludwig's Hand (URL-4).

Henri Becquerel discovered radioactivity while investigating the properties of uranium salts. His accidental discovery in 1896, along with the subsequent work of Marie and Pierre Curie, led to the identification of new radioactive elements, such as radium and polonium. Becquerel's early research on radioactivity opened up a new era in scientific exploration. His studies on the spontaneous emission of radiation from certain materials provided the groundwork for understanding the behavior of radioactive substances. The discovery of radium by the Curies and the understanding of its radioactive properties paved the way for medical applications. Radium became a key element in early cancer treatments, particularly in brachytherapy, where radium needles were used to irradiate tumors directly. Inspired by Becquerel's discoveries, Pierre Curie began using radium in cancer treatments. Brachytherapy, involving the

insertion of radium directly into tumors, became an early form of radiation therapy for certain cancers (Kattan et al., 2016).

Becquerel's work stimulated further research on artificial radioisotopes. This research, including the discovery of additional radioisotopes and their properties, expanded the range of materials available for medical applications. Becquerel's discoveries also contributed to advancements in external beam radiation therapy.

The use of external beam radiation for cancer treatment began in the early 20th century. Advances in linear accelerator technology and radiation delivery techniques improved the precision of radiation therapy.

The development of radioisotopes and scintillation detectors led to the establishment of nuclear medicine as a field. Technetium-99m, a widely used radioisotope, was discovered in the late 1930s, and by the 1950s, nuclear medicine procedures such as the gamma camera were in use.

Sir Godfrey Hounsfield and Allan Cormack developed the first CT scanner in 1970, which provided detailed cross-sectional images of the body. Since that date, CT scans became a powerful diagnostic tool in medical imaging. In 1990s, traditional film-based X-rays gradually transitioned to digital radiography, allowing for faster image acquisition, storage, and electronic sharing.

Throughout the history of radiation use in medicine, the field has continually evolved, with ongoing advancements enhancing diagnostic and therapeutic capabilities while prioritizing patient safety and minimizing radiation exposure (Kattan et al., 2016). As technology improved, radiation oncologists could deliver more precise and controlled doses of radiation to aim at cancerous cells. The use of radioisotopes and radiation-based imaging techniques in medicine, such as PET and SPECT, evolved over the years, providing clinicians with powerful tools for diagnosing various medical conditions.

2.4 Today's Radiation Use in Medicine

Radiation is greatly used in the field of medicine today for diagnostic and therapeutic objectives. X-rays are widely employed for imaging bones and detecting abnormalities in the chest, abdomen, and other body regions. CT imaging device use

X-rays to constitute detailed cross-sectional images of the body, providing enhanced diagnostic capabilities.

PET scans use radioactive tracers to detect changes in metabolic activity which is used in the diagnosis and monitoring of varied conditions. SPECT imaging involves the injection of radioactive substances to visualize organ function. Real-time X-ray imaging is used in interventional radiology for procedures such as angiography, stent placement, and catheter-based interventions. High-energy X-rays or other particles are directed at cancered tumors to eliminate or damage cancer cells. Radioactive sources are positioned directly within or close to tumors for targeted radiation therapy. Radioactive iodine (I-131) is used in treating thyroid conditions such as hyperthyroidism and thyroid cancer.

Systems are implemented to monitor and manage the radiation dose delivered during diagnostic imaging procedures, ensuring adherence to safety guidelines. Advanced imaging technologies, such as CT and MRI, play a crucial role in radiation therapy planning, allowing precise targeting of tumors while sparing healthy tissues. Molecular imaging techniques, such as PET, contribute to personalized medicine by providing information about specific molecular and cellular processes in the body (Kattan et al., 2016).

2.4.1 PET/CT devices

The PET/CT device is a medical imaging tool that bring together two advanced imaging techniques: PET and CT scans. PET detects the distribution of a radioactive tracer to highlight cellular activity, while CT provides detailed anatomical images. This fusion allows doctors to correlate metabolic data from PET with the precise anatomical location from CT, to monitore the medical conditions, especially cancer (Surti and Karp, 2016).

Medical imaging has witnessed significant advancements in recent years, with PET/CT devices standing at the forefront of diagnostic tools. These devices combine PET and CT imaging to provide extensive insights into the human body.

PET involves the injection of a small amount of a radioactive tracer, usually a form of glucose, into the patient’s body. Active cells, such as those in tumors, absorb and accumulate more of the tracer, emitting positrons in the process. CT imaging provides

precise anatomical information about the location and size of abnormalities via cross-sectional images of the body's internal structures.

The combination of PET and CT scan allows for the correlation of metabolic activity (from PET) with anatomical structures (from CT). This fusion enhances diagnostic accuracy and provides a more comprehensive understanding of the patient's condition. Figure 2.5 shows the difference of PET/CT devices and the combined device has a better imaging accuracy.

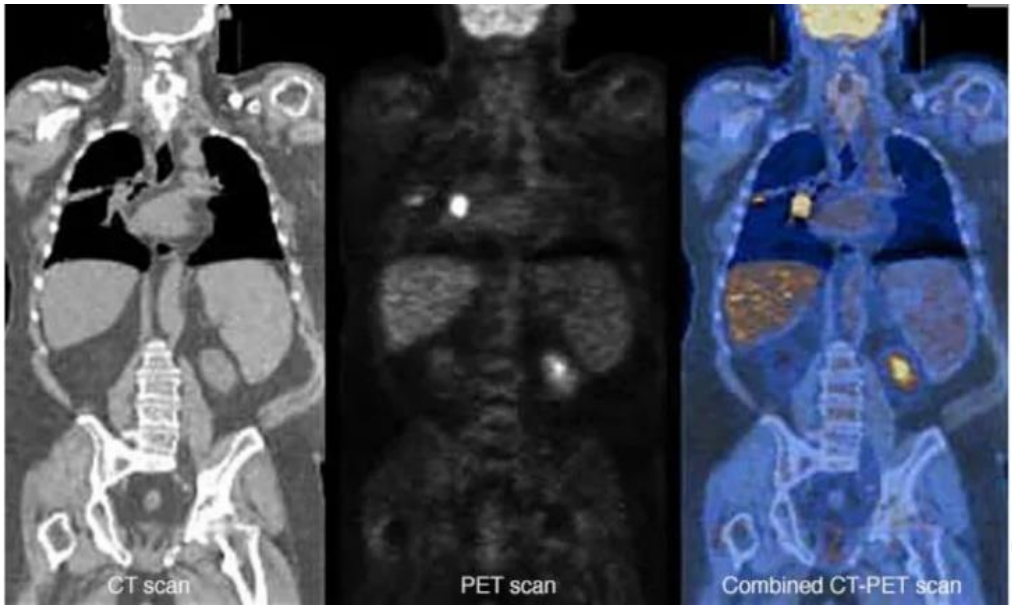

Figure 2.5 : Combined PET-CT Devices (URL-5).

This combined device is used in oncology for cancer detection, staging, and treatment planning. It also plays a crucial role in cardiology, neurology, and other fields, offering valuable insights into various diseases. Early detection of cancer and precise localization of abnormalities contribute to improved patient outcomes. PET/CT aids in monitoring treatment response and guiding therapeutic decisions.

Merging of PET and CT data provide a better sensitivity and specificity of the imaging process. This enhanced accuracy is particularly useful in determining small lesions and differentiating between benign and malignant conditions. PET/CT is precious in treatment planning, especially in radiation therapy and surgery, where knowing the exact location of abnormalities is critical.

It aids in monitoring treatment response over time, allowing for adjustments to the therapeutic approach based on changes in metabolic activity and anatomical features. Integrating PET and CT information helps reduce false positives and negatives that

may occur when interpreting results from each modality separately. The combined data set improves the overall reliability of the diagnostic process. Performing PET and CT scans in a single session streamlines the imaging process and minimizes the need for separate appointments. This is convenient for both patients and healthcare providers, saving time and resources. (Surti and Karp, 2016).

2.4.2 Radiopharmaceuticals

Radiopharmaceuticals are composed of radionuclide and pharmaceutical compound. These two components work together to create a radiopharmaceutical that can be administered to human body for diagnostic imaging or therapeutic purposes. The radionuclide is the radioactive component of the radiopharmaceutical. It emits radiation in the form of gamma rays or positrons. The combination of a radioactive component with a pharmaceutical compound allows for the localization and visualization of physiological processes within the body (Mettler and Guiberteau, 2018). The choice of radionuclide depends on the specific medical application and the characteristics required for imaging or therapy. Radiopharmaceuticals are given to patients through various ways, including oral ingestion, intravenous injection, or inhalation, depending on the specific radiopharmaceutical and the medical procedure being performed (Dash, 2011).

The pharmaceutical compound is the non-radioactive part of the radiopharmaceutical. It is a chemical compound or molecule that is combined with the radionuclide to form a functional and biologically active agent. The pharmaceutical compound determines the biological behavior, specificity, and targeting of the radiopharmaceutical within the body. Different pharmaceutical compounds are selected based on the organ or tissue of interest and the medical purpose (diagnosis or therapy).

Radiopharmaceuticals used in PET/CT act as tracers for molecular imaging. These compounds are designed to target specific biological processes or molecules within the body, providing insights into cellular activity, metabolism, and organ function at the molecular level. PET relies on the detection of positron emissions from the administered radiopharmaceuticals. When the radiopharmaceutical undergoes radioactive decay, it emits positrons, which subsequently annihilate with nearby electrons, resulting in the release of two gamma rays. PET detectors pick up these gamma rays, enabling the creation of functional images.

Radiopharmaceuticals in PET/CT serve as powerful diagnostic tools, aiding in the detection and staging of diseases such as cancer. By visualizing metabolic activity and identifying areas of increased cellular turnover, PET/CT helps clinicians evaluate the extent and characteristics of diseases.

PET/CT devices are used to monitor the reaction to therapy. Changes in metabolic activity after treatment can be observed, guiding clinicians in assessing the effectiveness of interventions and making informed decisions about ongoing care.

In therapeutic applications, PET/CT with certain radiopharmaceuticals assists in dosimetry for radiation therapy planning. It helps determine the distribution of the radiopharmaceutical within the target tissue, optimizing treatment strategies. Radiopharmaceuticals in PET/CT contribute to research and drug development. They enable scientists to investigate molecular processes, study disease mechanisms, and assess the efficacy of new drugs at the molecular level.

2.4.2.1 ^{18}F-FDG

^{18}F-FDG, or fluorodeoxyglucose labeled with Fluorine-18, is a radiopharmaceutical widely used in PET imaging to visualize and assess metabolic activity within the body. Fluorodeoxyglucose (FDG) is a glucose analog in which a radioactive isotope of fluorine, specifically Fluorine-18 (F-18), is substituted for a hydroxyl group. Glucose is a natural source of energy for cells, and FDG mimics glucose in the body.

Fluorine-18 (F-18) is a positron-emitting isotope, meaning it releases positively charged particles called positrons during radioactive decay. This property makes F-18 suitable for PET imaging, as the emitted positrons can be detected and used to create detailed images of metabolic processes in tissues (Dash, 2011).

^{18}F-FDG is typically administered to the patient through intravenous injection. Cancer cells has high metabolic activity, and these cells take up ^{18}F-FDG because they use glucose more rapidly than normal cells. This increased uptake is due to the similarity between FDG and natural glucose. Once inside the cells, F-18 undergoes radioactive decay by emitting positrons. Positrons are short-lived particles that quickly encounter electrons. When a positron encounters an electron, both particles annihilate, emitting two gamma rays in opposite directions. PET scanners detect these gamma rays, and the information is used to create detailed three-dimensional images depicting the distribution of ^{18}F-FDG in the body.

^{18}F-FDG PET imaging is widely used for various clinical purposes, including those identifying areas of increased metabolic activity helps in detecting and staging cancers. Assessing the response of tumors to treatments like chemotherapy or radiation therapy.

In oncology, FDG is used for colorectal cancer, non-small cell lung cancer, lymphoma, malignant melanoma, esophagea, head and neck, thyroid and breast cancer. ^{18}F-FDG PET imaging provides valuable insights into the metabolic activity of tissues and is one of the most essential tools in nuclear medicine (Dash, 2011).

2.4.2.2 ^{68}Ga-PSMA

^{68}Ga-PSMA (gallium-68 prostate-specific membrane antigen) is a radiotracer used in PET imaging device to detect and stage the prostate cancer. This imaging technique, often referred to as ^{68}Ga-PSMA PET, targets the PSMA, a cell surface protein that is described in prostate cancer cells.

Ga-68, a positron-emitting radionuclide, is attached to a ligand that specifically binds to PSMA as radiotracer labelling. Common ligands used for ^{68}Ga-PSMA PET include PSMA-11 (also known as HBED-CC) and PSMA I&T. During ^{68}Ga-PSMA PET imaging, a radiotracer is injected into the bloodstream, selectively binding to PSMA on prostate cancer cells' surfaces. This technique has shown sensitivity and specificity in identifying both primary and metastatic prostate cancer lesions. It is particularly valuable in cases where prostate-specific antigen (PSA) levels are elevated, and conventional imaging methods may not provide sufficient information.

The application of ^{68}Ga-PSMA PET has rapidly evolved, and it has become a crucial tool in prostate cancer management, providing valuable information for clinicians to make informed decisions about patient care (Mettler and Guiberteau, 2018). It enhances diagnostic accuracy, facilitates precise staging, and contributes to personalized treatment strategies for individuals diagnosed with prostate cancer.

^{68}Ga-PSMA PET is used for various clinical applications in prostate cancer, including identifying the extent of the disease in the prostate and nearby lymph nodes. It is used to detect the recurrence of prostate cancer based on rising PSA levels after initial treatment. ^{68}Ga-PSMA PET is often part of a theranostic approach. After imaging, if the cancer is detected or localized, the same PSMA targeting can be used for therapeutic interventions, such as Lutetium-177 PSMA radionuclide therapy.

3. METHOD

Effective dose (ED) from PET and CT both are calculated and combined to represent a whole body burden by the following equation (Abuqbeitah et al., 2023):

$$\text{Total ED} = \text{ED from PET part} + \text{ED from CT part} \quad (3.1)$$

3.1 Effective Dose from PET

In nuclear medicine, estimating radiation absorbed doses during diagnostic procedures include calculations using models of the human body and the biokinetic data of the radiopharmaceutical.

3.1.1 Biokinetic data

Biokinetic data refers to information and data related to the movement, distribution, and elimination of a substance, such as a drug or a radioactive tracer, within a biological system. The term “biokinetics’’ is derived from “bio’’ (life) and “kinetics’’ (movement), emphasizing the study of how substances move and behave within living organisms (Powsner et al., 2013).

Biokinetic data is crucial in various scientific disciplines, including pharmacology, toxicology, and nuclear medicine. It provides insights into the absorption, distribution, metabolism, and excretion of substances in the body. Understanding the biokinetics of a substance is essential for assessing its safety, efficacy, and potential impact on human health. In nuclear medicine and radiopharmaceuticals, biokinetic data is particularly important for:

Dosimetry: Determining the radiation dose delivered to specific organs and tissues following the injection of a radioactive substance.

Imaging Interpretation: Understanding how a radiotracer is taken up, distributed, and cleared within the body helps in the interpretation of medical imaging studies, such as PET and SPECT.

Radiation Protection: Evaluating the radiation exposure to patients and healthcare workers is essential for guaranteeing that radiation doses are kept within ALARA exposure limits. Biokinetic models help estimate the amount of radiation absorbed by different organs.

Pharmacokinetics: In pharmacology, biokinetic data is used to study the movement and fate of drugs within the body. This information is crucial for determining optimal dosage regimens and predicting the therapeutic effects of drugs.

Biokinetic data is often obtained through a combination of experimental studies, clinical trials, and mathematical modeling. Radiotracer studies, blood and urine sampling, and imaging techniques contribute to the collection of data that can be used to develop biokinetic models. These models explain the behavior of a substance in the human body over time, providing a quantitative understanding of its kinetics.

Overall, biokinetic data plays a fundamental role in advancing our understanding of how substances interact with living systems, guiding the development and application of drugs, diagnostic agents, and therapeutic interventions (Stabin, 2007). Table 3.1 shows the biokinetic data of F-18 taken from ICRP 128 and Table 3.2 shows the biokinetic data of Ga-68 taken from the literature (Demirci et al., 2018).

Table 3.1 : Biokinetic data for F-18 (ICRP 128, 2015).

Organ(S)	F_S	T(h)	A	A_s/A_0 (h)
Brain	0.08	∞	1.0	0.21
Heart wall	0.04	∞	1.0	0.11
Lungs	0.03	∞	1.0	0.079
Liver	0.05	∞	1.0	0.13
Other organs and tissues	0.80	0.20	0.075	1.7
		1.50	0.225	
		∞	0.70	
Urinary bladder contents	0.24			
Adult, 15 years, 10 years				0.26
5 years				0.23
1 year				0.16

Table 3.2 : Biokinetic data for Ga-68 (Demirci et al., 2018).

Organ	Patient 1	Patient 2	Patient 3	Patient 4	Patient 5	Patient 6	Patient 7	Mean±SEM
Lacmiral-R	1.72E-04	2.47E-04	1.23E-04	1.67E-04	6.83E-05	1.85E-04	1.89E-05	1.40E-04 ± 0.03E-04
Lacmiral-L	1.63E-04	1.77E-04	9.09E-05	1.59E-04	6.68E-05	1.79E-04	2.23E-05	1.20E-04 ± 0.02E-04
SubMand-R	1.35E-03	3.55E-03	8.40E-04	1.62E-03	1.45E-03	4.20E-03	5.70E-04	0.002 ± 0.000
SubMand-L	1.37E-03	3.35E-03	1.05E-03	1.27E-03	1.96E-03	-*[3]	8.80E-04	0.002 ± 0.000
Parotid G-R	3.29E-03	3.90E-03	2.26E-03	-*[3]	3.80E-03	6.50E-03	1.50E-03	0.004 ± 0.001
Parotid G-L	4.26E-03	5.68E-03	1.84E-03	3.01E-03	3.65E-03	5.90E-03	1.70E-03	0.004 ± 0.001
Böbrek-R	8.30E-02	1.28E-01	1.17E-01	8.90E-02	3.00E-02	8.75E-02	6.70E-02	0.086 ± 0.011
Böbrek-L	7.20E-02	1.52E-01	1.86E-01	7.70E-02	2.80E-02	7.50E-02	4.60E-02	0.091 ± 0.020
Liver	-*[1]	1.06E-01	7.40E-02	8.60E-02	8.30E-02	6.14E-02	2.48E-01	0.110 ± 0.024
Spleen	8.32E-03	1.07E-02	7.25E-03	9.50E-03	2.00E-02	1.70E-02	9.10E-03	0.012 ± 0.002
Bladder	1.06E-01	4.95E-02	1.76E-01	3.50E-02	3.70E-02	5.70E-02	2.90E-02	0.070 ± 0.019
Lomber vert.	-*[2]	5.28E-03	2.07E-03	2.04E-03	4.25E-03	2.44E-03	4.43E-03	0.003 ± 0.000
Bone marrow	-*[2]	7.88E-02	3.09E-02	3.04E-02	6.34E-02	3.64E-02	6.61E-02	0.051 ± 0.007
Remaining body	5.09E-01	2.57E-01	1.92E-01	4.63E-01	5.61E-01	5.45E-01	3.14E-01	0.406 ± 0.052

*Marked values cannot be calculated due to multiple liver metastasis (1), bone metastasis (2) and adjacent tumor (3).

3.1.2 MIRD methodology

The MIRD (Medical Internal Radiation Dose) method is a systematic approach in nuclear medicine to calculate the radiation absorbed dose in different organs and tissues of the human body after administering radiopharmaceuticals. It was developed by the Society of Nuclear Medicine and Molecular Imaging (SNMMI) Committee on Radiation Dosimetry.

MIRD involves the use of mathematical models to explain the biodistribution and kinetics of radiopharmaceuticals within the body. These models take into account factors such as uptake, distribution, and clearance of the radiotracer by different organs and tissues. The MIRD method often includes studies using phantoms, which are physical or mathematical representations of the human body. These studies help validate the mathematical models and provide a basis for estimating radiation doses in various organs. Figure 3.1 shows the phantom used in MIRD method taken from ICRP 23.

The primary objective of the MIRD method is to determine the absorbed dose in different tissues due to the emission of ionizing radiation from radionuclides within radiopharmaceuticals. This information is crucial for understanding the potential biological effects of the radiation exposure. MIRD provides standardized data for various radiopharmaceuticals, allowing for consistent and comparable dose estimates across different studies and medical centers. MIRD-based dose estimates are often reported in units such as milligray (mGy) or millisievert (mSv) and are used to assess radiation risk and guide practitioners in optimizing imaging and therapeutic procedures. The MIRD method is applied in both diagnostic and therapeutic nuclear medicine. In diagnostic applications, it helps estimate radiation doses from imaging studies using radiopharmaceuticals. In therapeutic applications, MIRD is used to predict the absorbed doses delivered to target organs and non-target organs in radionuclide therapy.

The MIRD Committee continues to work on refining and expanding the method, incorporating advancements in imaging technology, radiopharmaceutical development, and dosimetric modeling. The MIRD method has become a standard approach in nuclear medicine for estimating radiation dose (Attix, 1986).

There are some certain terms that clarify the internal radiation calculation through MIRD method as stated below.

Source Area

A region where a radiopharmaceutical remains for a specific duration, correlated with the drug's biological half-life, and emits ionizing radiation to surrounding areas.

Target Area

Area exposed to ionizing radiation from source area.

Cumulative Activity

Creating a time-activity curve involves plotting activity levels at various time points after injection over time. Integrating this curve enables to obtain the cumulative activity in a specific organ, a significant parameter that needs to be calculated for each patient.

S value

Absorbed dose in the target area per unit of cumulative radioactivity in the source area.

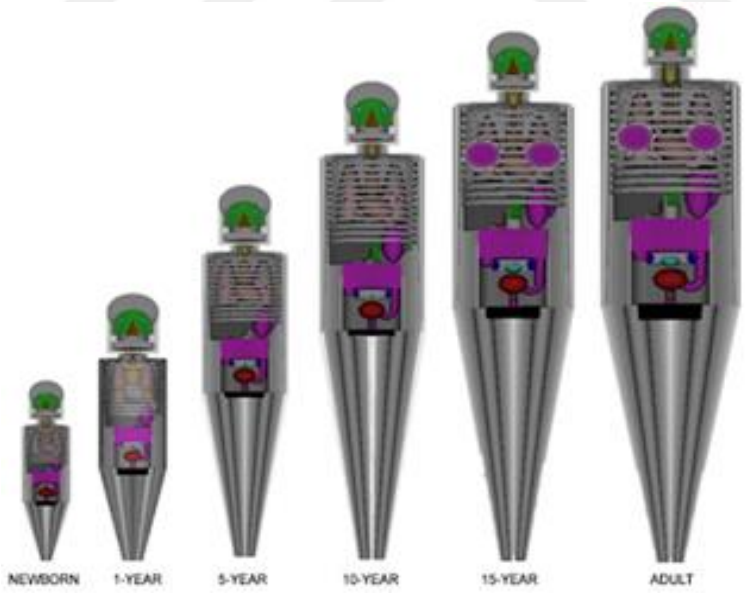

Figure 3.1 : MIRD Phantom (ICRP 23, 1975).

The MIRD method employs a simple model of the human body, designating organs as source organs, containing the radiopharmaceutical, and target organs, where the absorbed dose is computed. Furthermore, an organ can serve as both a source and a target in this approach (Attix, 1986). The MIRD method consists of the following steps.

Step 1. Compute accumulated activity

Accumulated activity (A_s) is influenced by both the administered activity (A_0) and the fraction of that activity absorbed by the source organ (F_s). It is calculated based on these factors at a specific point in time as following:

$$A_s(t) = A_0 F_s e^{-\lambda_e t} \tag{3.2}$$

Here, λ_e represents the effective decay constant.

The effective half-life combined the physical half-life and the biological half-life. In contrast, the effective decay constant (λ_e) represents the rate of decay, encompassing both physical and biological processes. These parameters provide a comprehensive understanding of how long a radionuclide is remaining throughout the body and its decay characteristics. Effective half life and effective decay constant are defined as:

$$\frac{1}{t_{1/2(effective)}} = \frac{1}{t_{1/2(physical)}} + \frac{1}{t_{1/2(biological)}} \tag{3.3}$$

$$\lambda_{effective} = \lambda_{physical} + \lambda_{biological} \tag{3.4}$$

Where $t_{1/2}$ is half life and λ is decay constant.

Step 2. Determine the S-factor

The S-factor, measuring the mean dose per unit of activity, is stated in units of Gy/Bq×s. While it can be calculated, it is commonly available in tables, dependent on the specific radionuclide, source organ, and target organ. The calculations utilize the MIRD phantom, representing a simplified model of a 70 kg adult male.

Step 3. Compute dose to the target organ

Dose to the target organ (D) is calculated from accumulated activity (A_s) and *S* factor.

$$\overline{D} = A_S \, x \, S \tag{3.5}$$

Step 4. Compute effective dose to the whole body

Effective dose (*ED*) may be calculated as following:

$$ED = \sum w_T H_T \tag{3.6}$$

Where,

w_T: tissue weighting factor

H_T: Equivalent dose.

3.1.3 OLINDA and IDAC software programs

In radiological protection, the Dose and Risk Calculation (DCAL) program is employed for radionuclides entering human body through inhalation and ingestion in environmental and occupational exposures. This program allows the derivation of nuclide-specific dose coefficients, which are published by ICRP.

OLINDA (Organ Level INternal Dose Assessment) and IDAC (Internal Dose Assessment by Computer) are softwares used in nuclear medicine for the evaluation and calculation of internal radiation doses sourcing from the administration of radiopharmaceuticals. These programs help estimate the absorbed doses to various tissues, providing valuable information for both diagnostic and therapeutic applications.

Both OLINDA and IDAC play essential roles in nuclear medicine dosimetry. They are valuable tools for researchers, radiologists, and medical physicists involved in assessing and managing radiation doses associated with the use of radiopharmaceuticals. These softwares contribute to the optimization of imaging and therapy procedures, ensuring the safe and effective application of nuclear medicine techniques (Ramos et al., 2017).

3.1.3.1 IDAC

The IDAC-Dose2.1 internal dosimetry computer program was created in accordance with ICRP guidelines and computational frameworks outlined in ICRP 133. This program is designed to estimate internal radiation doses in reference adults.

The main objective of IDAC-Dose is to provide a standardized and accurate method for estimating internal radiation doses. It is particularly valuable in assessing the radiation exposure resulting from the use of radionuclides in diagnostic imaging studies and targeted radionuclide therapies. IDAC-Dose likely employs mathematical models and biokinetic data to simulate the biodistribution and retention of radionuclides within the human body. These models take into account factors such as radionuclide decay, organ uptake, and clearance pathways.

The IDAC-Dose2.1 program utilize radionuclide decay data from ICRP Publication 107, encompassing 83 source regions affecting 47 target tissues. Tissue weighting

factors from ICRP Publications 60 and 103 are incorporated to compute the effective dose. The software's validation against DCAL program, using the same computational framework, ensures accuracy and reliability.

Additionally, IDAC-Dose2.1 features a sub-module for absorbed dose calculations in spherical structures of varying volumes and composition, specifically designed for estimating absorbed doses in radiopharmaceutical therapy. The calculations also include contributions from decay products for nine specific alpha emitters in committed absorbed dose assessments (Andersson et al., 2017).

Absorbed dose estimations were directly derived from Monte Carlo simulations, using the adult reference computational phantoms described in ICRP 110 (Andersson et al., 2017) Furthermore, IDAC Software allows the user calculate the effective dose based on the old phantom described in ICRP 23 too. This feature enables the healthcare workers to estimate radiation exposure depended on phantoms used in quantative way for both two different quidelines of ICRP Publication. Phantom described in ICRP 23 have been showed in Figure 3.1 in the section 3.1.2.

The ICRP employed voxel models for their computational phantoms, specifically the Reference Computing Phantoms of the Human Body Adult Male (RCP-AM) and Female (RCP-AF) as published in ICRP 110. These phantoms, representing both sexes, were constructed from real human body CT data. The geometries, sizes, compositions, and densities of organs and tissues of ICRP Publication 110 were shown in Figure 3.2 and Figure 3.3 (ICRP 110, 2009).

Figure 3.4 shows the IDAC-Dose2.1 interface of the biokinetic data registered for ^{18}F-FDG and Figure 3.5 shows the ^{18}F-FDG absorbed doses per unit activity for the selected target organs for new phantom.

Absorbed doses per unit activity calculated by IDAC old phantom as presented in ICRP 23 and tissue weighting factors as presented in ICRP 60 guidelines were given in Figure 3.6. While there is gender discrimination in ICRP 60 guideline, it was expected that male and female results would come out separately, but since there is no gender discrimination in old phantom, we used absorbed dose per unit activity of the 15-year-old child patient to calculate the dose of the female patient.

Figure 3.2 : ICRP-110 reference phantoms (ICRP 110; 2009).

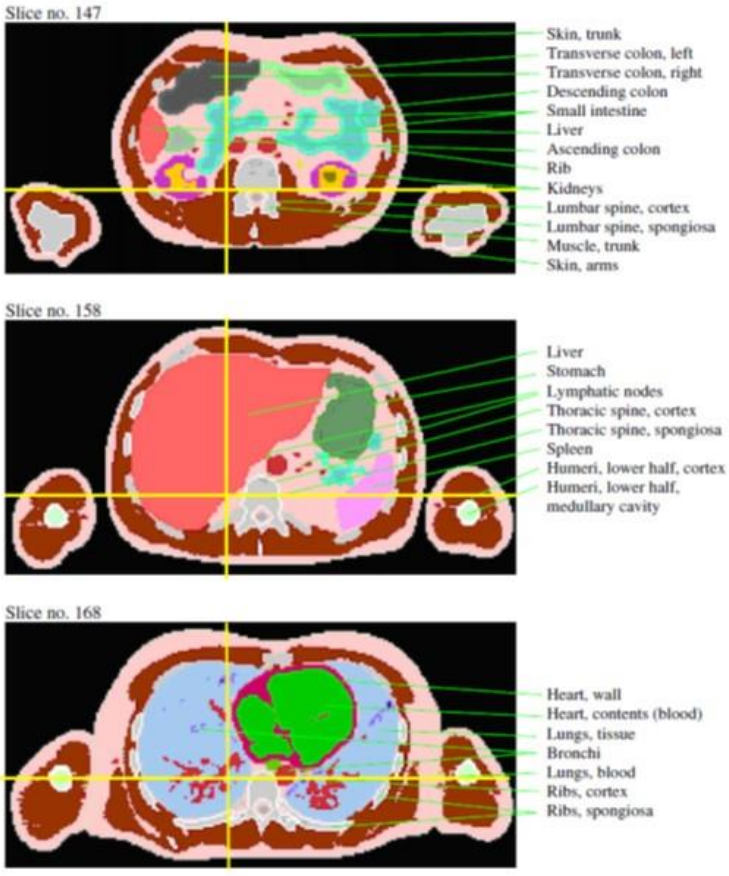

Figure 3.3 : ICRP 110 reference phantom (geometries and sizes of the organs) (ICRP 110, 2009).

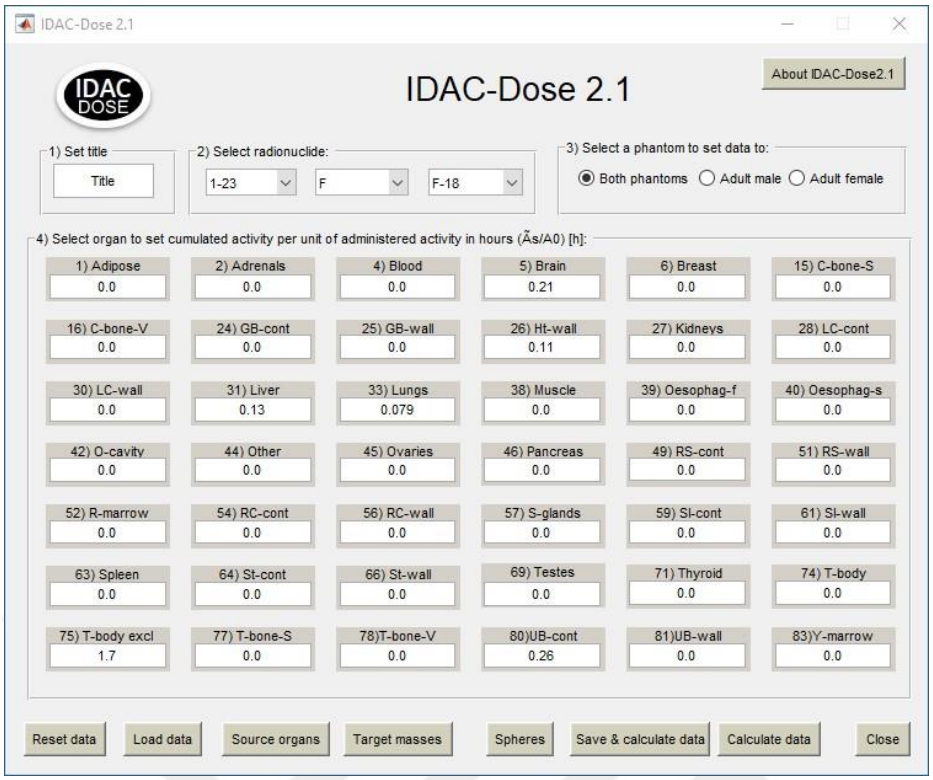

Figure 3.4 : IDAC biokinetic data interface for ^{18}F-FDG.

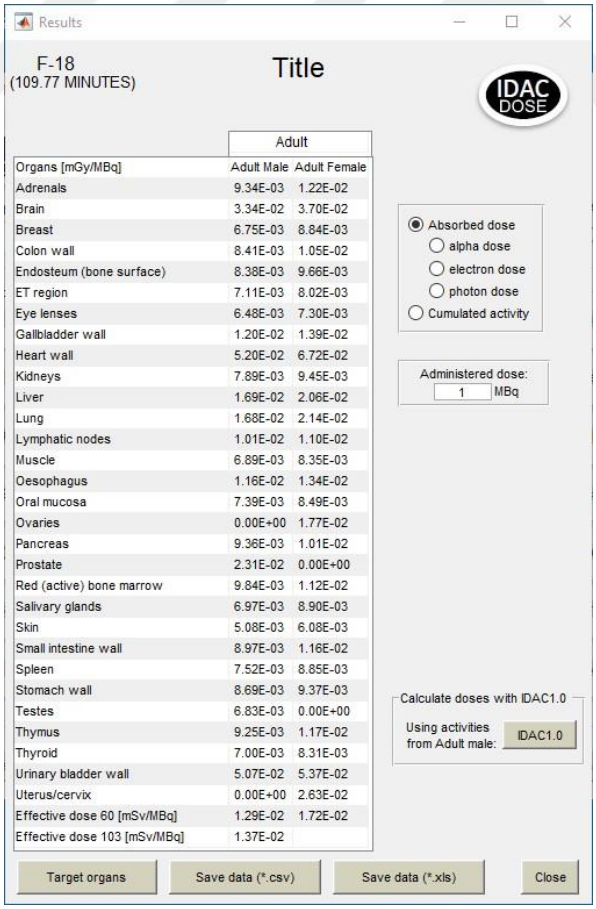

Figure 3.5 : Absorbed doses per unit activity for ^{18}F-FDG (new phantom).

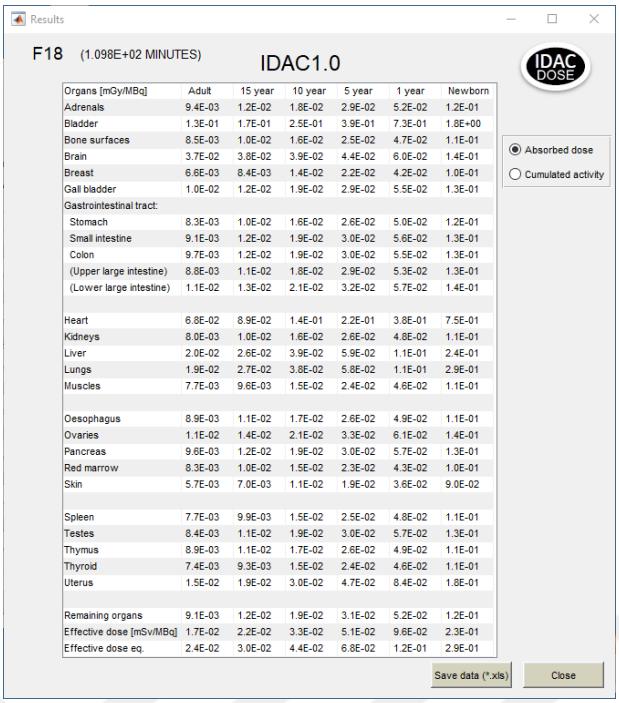

Organs [mGy/MBq]	Adult	15 year	10 year	5 year	1 year	Newborn
Adrenals	9.4E-03	1.2E-02	1.8E-02	2.9E-02	5.2E-02	1.2E-01
Bladder	1.3E-01	1.7E-01	2.5E-01	3.9E-01	7.3E-01	1.8E+00
Bone surfaces	8.5E-03	1.0E-02	1.6E-02	2.5E-02	4.7E-02	1.1E-01
Brain	3.7E-02	3.8E-02	3.9E-02	4.4E-02	6.0E-02	1.4E-01
Breast	6.6E-03	8.4E-03	1.4E-02	2.2E-02	4.2E-02	1.0E-01
Gall bladder	1.0E-02	1.2E-02	1.9E-02	2.9E-02	5.5E-02	1.3E-01
Gastrointestinal tract:						
Stomach	8.3E-03	1.0E-02	1.6E-02	2.6E-02	5.0E-02	1.2E-01
Small intestine	9.1E-03	1.2E-02	1.9E-02	3.0E-02	5.6E-02	1.3E-01
Colon	9.7E-03	1.2E-02	1.9E-02	3.0E-02	5.5E-02	1.3E-01
(Upper large intestine)	8.8E-03	1.1E-02	1.8E-02	2.9E-02	5.3E-02	1.3E-01
(Lower large intestine)	1.1E-02	1.3E-02	2.1E-02	3.2E-02	5.7E-02	1.4E-01
Heart	6.8E-02	8.9E-02	1.4E-01	2.2E-01	3.8E-01	7.5E-01
Kidneys	8.0E-03	1.0E-02	1.6E-02	2.6E-02	4.8E-02	1.1E-01
Liver	2.0E-02	2.6E-02	3.9E-02	5.9E-02	1.1E-01	2.4E-01
Lungs	1.9E-02	2.7E-02	3.8E-02	5.8E-02	1.1E-01	2.9E-01
Muscles	7.7E-03	9.6E-03	1.5E-02	2.4E-02	4.6E-02	1.1E-01
Oesophagus	8.9E-03	1.1E-02	1.7E-02	2.6E-02	4.9E-02	1.1E-01
Ovaries	1.1E-02	1.4E-02	2.1E-02	3.3E-02	6.1E-02	1.4E-01
Pancreas	9.6E-03	1.2E-02	1.9E-02	3.0E-02	5.7E-02	1.3E-01
Red marrow	8.3E-03	1.0E-02	1.5E-02	2.3E-02	4.3E-02	1.0E-01
Skin	5.7E-03	7.0E-03	1.1E-02	1.9E-02	3.6E-02	9.0E-02
Spleen	7.7E-03	9.9E-03	1.5E-02	2.5E-02	4.8E-02	1.1E-01
Testes	8.4E-03	1.1E-02	1.9E-02	3.0E-02	5.7E-02	1.3E-01
Thymus	8.9E-03	1.1E-02	1.7E-02	2.6E-02	4.9E-02	1.1E-01
Thyroid	7.4E-03	9.3E-03	1.5E-02	2.4E-02	4.6E-02	1.1E-01
Uterus	1.5E-02	1.9E-02	3.0E-02	4.7E-02	8.4E-02	1.8E-01
Remaining organs	9.1E-03	1.2E-02	1.9E-02	3.1E-02	5.2E-02	1.2E-01
Effective dose [mSv/MBq]	1.7E-02	2.2E-02	3.3E-02	5.1E-02	9.6E-02	2.3E-01
Effective dose eq.	2.4E-02	3.0E-02	4.4E-02	6.8E-02	1.2E-01	2.9E-01

Figure 3.6 : Absorbed doses per unit activity for ^{18}F-FDG (old phantom).

The biokinetic data and absorbed dose per unit activity interfaces used for ^{68}Ga-PSMA in this study are shown in Figure 3.7 and Figure 3.8 respectively.

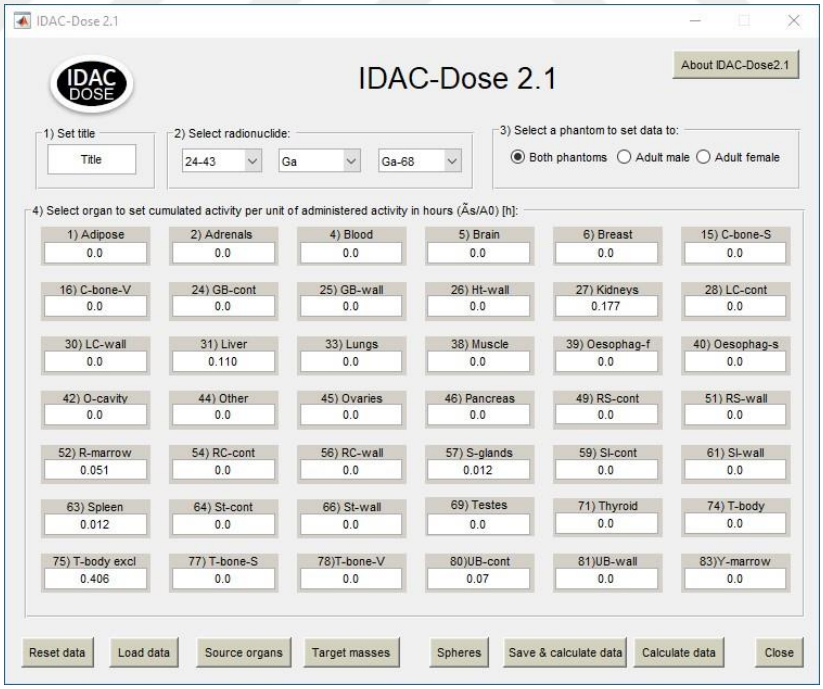

Figure 3.7 : IDAC biokinetic data interface for ^{68}Ga-PSMA

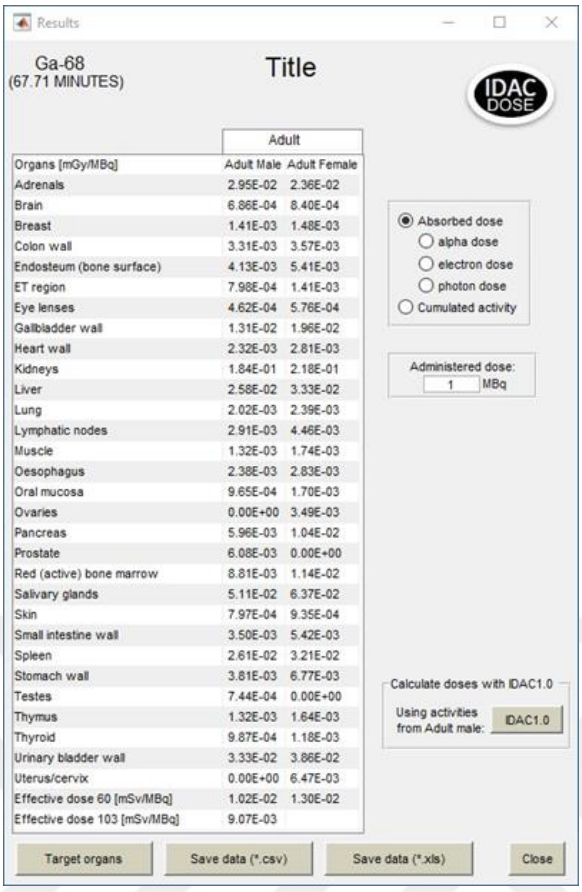

Figure 3.8 : IDAC absorbed dose per unit activity interface for ^{68}Ga-PSMA.

3.1.3.2 OLINDA/EXM

OLINDA/EXM, which stands for Organ Level Internal Dose Assessment/EXponential Modeling uses MIRD methodology is an upgrade of MIRDose, a program for calculating internal radiation dose estimation in nuclear medicine.

This code provides nuclear medicine dose factors for a broader spectrum of nuclides (over 1000 compared to 117 in MIRDose), encompassing alpha emitters as well. It uses second-generation voxel-based realistic phantoms designed for adults, children, and pregnant women, adhering to reference organ masses defined by ICRP 89.

Additionally, it includes some animal models such as mice, rats, and dogs. The program allows for the adjustment of organ masses to patient-specific values and the assignment of activity to the walls of hollow organs. In OLINDA/EXM code segment, users are able to conduct kinetic analyses, fitting sums of exponentials to data collected in human body or animal studies (Ramos et al., 2017).

In the 1960s, OLINDA/EXM software utilizes phantoms grounded in stylized anatomical models created by the MIRD. These models mathematically represent

organs using descriptive and schematic materials from general anatomy references. They adhere to the recommendation of the 'Reference Man' described by ICRP 23 which is published in 1975 and the phantom have been showed in Figure 3.1 (Lacerda et al., 2020).

The biokinetic data and absorbed dose per unit activity interfaces for ^{18}F-FDG used in this study are given in Figure 3.9 and Figure 3.10 respectively.

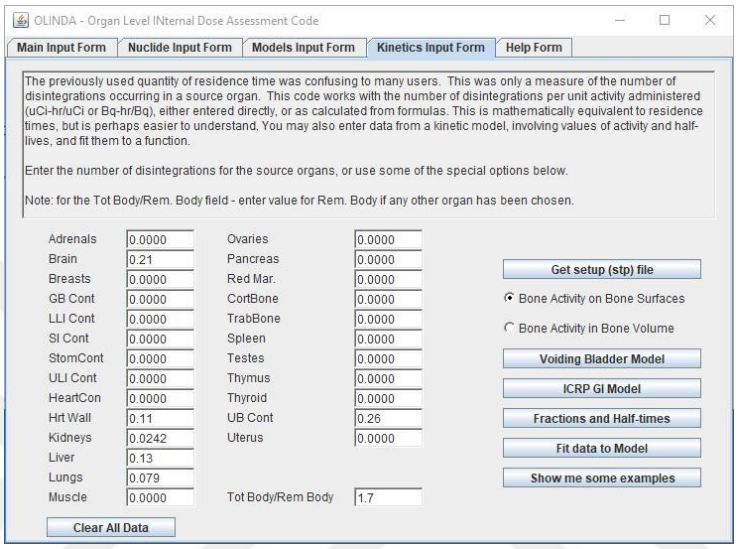

Figure 3.9 : OLINDA Biokinetic Data interface for ^{18}F-FDG.

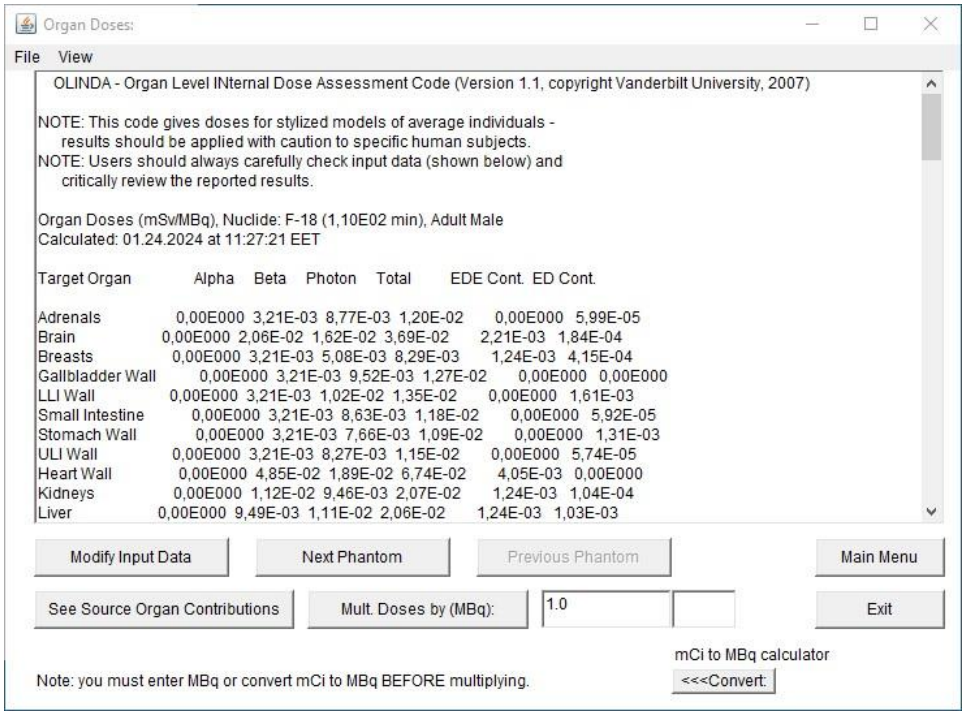

Figure 3.10 : OLINDA absorbed dose per unit activity interface for ^{18}F-FDG.

The biokinetic data and absorbed dose per unit activity interfaces for ^{68}Ga-PSMA used in this study can be seen in Figure 3.11 and Figure 3.12 respectively.

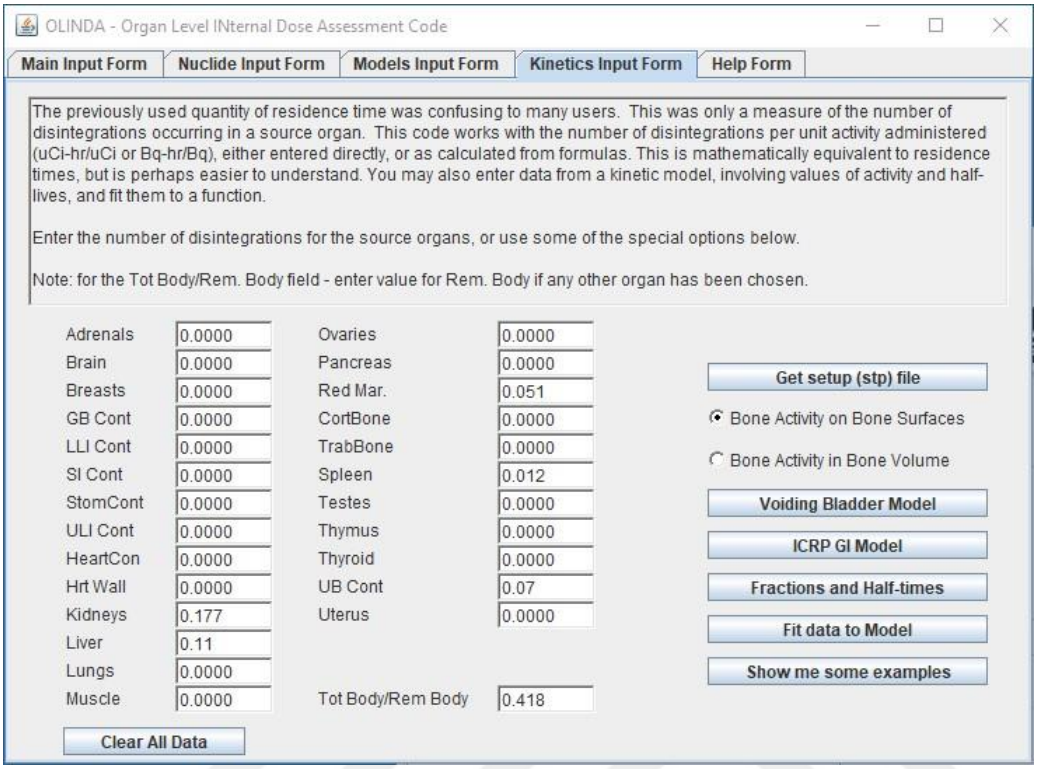

Figure 3.11 : OLINDA Biokinetic Data interface for ^{68}Ga-PSMA.

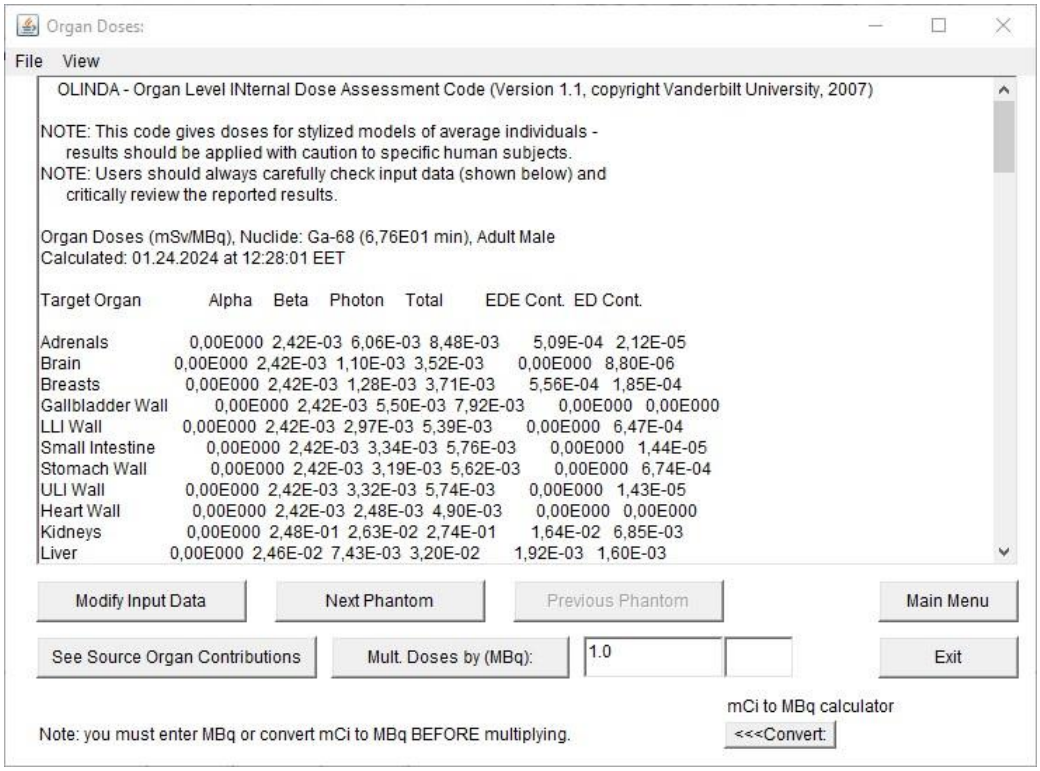

Figure 3.12 : OLINDA absorbed dose per unit activity interface for ^{68}Ga-PSMA.

Furthermore, OLINDA result page is not as clear as IDAC page as it is the previous software program for the internal radiation dose calculation. Calculated results page on OLINDA have been exported to excel page to make the data more understandable. Table 3.3 and Table 3.4 shows the male and female patient results separately for ^{18}F-FDG exported to excel page. Table 3.5 shows the male patient results for ^{68}Ga-PSMA.

Table 3.3 : Male patient results for ^{18}F-FDG on excel page.

Target Organ	Alpha	Beta	Photon	Total	EDE Cont.	ED Cont.
Adrenals	0.00E+00	3.21E-03	8.77E-03	1.20E-02	0.00E+00	5.99E-05
Brain	0.00E+00	2.06E-02	1.62E-02	3.69E-02	2.21E-03	1.84E-04
Breasts	0.00E+00	3.21E-03	5.08E-03	8.29E-03	1.24E-03	4.15E-04
Gallbladder Wall	0.00E+00	3.21E-03	9.52E-03	1.27E-02	0.00E+00	0.00E+00
LLI Wall	0.00E+00	3.21E-03	1.02E-02	1.35E-02	0.00E+00	1.61E-03
Small Intestine	0.00E+00	3.21E-03	8.63E-03	1.18E-02	0.00E+00	5.92E-05
Stomach Wall	0.00E+00	3.21E-03	7.66E-03	1.09E-02	0.00E+00	1.31E-03
ULI Wall	0.00E+00	3.21E-03	8.27E-03	1.15E-02	0.00E+00	5.74E-05
Heart Wall	0.00E+00	4.85E-02	1.89E-02	6.74E-02	4.05E-03	0.00E+00
Kidneys	0.00E+00	1.12E-02	9.46E-03	2.07E-02	1.24E-03	1.04E-04
Liver	0.00E+00	9.49E-03	1.11E-02	2.06E-02	1.24E-03	1.03E-03
Lungs	0.00E+00	1.10E-02	8.33E-03	1.93E-02	2.32E-03	2.32E-03
Muscle	0.00E+00	3.21E-03	6.59E-03	9.80E-03	0.00E+00	4.90E-05
Ovaries	0.00E+00	3.21E-03	1.03E-02	1.36E-02	3.39E-03	2.71E-03
Pancreas	0.00E+00	3.21E-03	9.10E-03	1.23E-02	0.00E+00	6.16E-05
Red Marrow	0.00E+00	2.29E-03	7.41E-03	9.70E-03	1.16E-03	1.16E-03
Osteogenic Cells	0.00E+00	6.90E-03	7.65E-03	1.45E-02	4.36E-04	1.45E-04
Skin	0.00E+00	3.21E-03	4.18E-03	7.39E-03	0.00E+00	7.39E-05
Spleen	0.00E+00	3.21E-03	7.15E-03	1.04E-02	0.00E+00	5.18E-05
Testes	0.00E+00	3.21E-03	7.34E-03	1.06E-02	0.00E+00	0.00E+00
Thymus	0.00E+00	3.21E-03	7.85E-03	1.11E-02	0.00E+00	5.53E-05
Thyroid	0.00E+00	3.21E-03	6.41E-03	9.62E-03	2.89E-04	4.81E-04
Urinary Bladder Wall	0.00E+00	8.91E-02	4.29E-02	1.32E-01	7.92E-03	6.60E-03
Uterus	0.00E+00	3.21E-03	1.48E-02	1.80E-02	0.00E+00	8.99E-05
Total Body	0.00E+00	4.32E-03	6.96E-03	1.13E-02	0.00E+00	0.00E+00

PET effective dose per unit activity (mSv/MBq) was calculated as 1.86E-02 for male patients administered ^{18}F-FDG radiopharmaceutical by OLINDA software.

Table 3.4 : Female patient results for ^{18}F-FDG on excel page.

Target Organ	Alpha	Beta	Photon	Total	EDE Cont.	ED Cont.
Adrenals	0.00E+00	4.16E-03	1.08E-02	1.50E-02	0.00E+00	7.50E-05
Brain	0.00E+00	2.44E-02	1.80E-02	4.24E-02	2.55E-03	2.12E-04
Breasts	0.00E+00	4.16E-03	6.41E-03	1.06E-02	1.59E-03	5.29E-04
Gallbladder Wall	0.00E+00	4.16E-03	1.10E-02	1.51E-02	0.00E+00	0.00E+00
LLI Wall	0.00E+00	4.16E-03	1.29E-02	1.70E-02	0.00E+00	2.04E-03
Small Intestine	0.00E+00	4.16E-03	9.74E-03	1.39E-02	0.00E+00	6.95E-05
Stomach Wall	0.00E+00	4.16E-03	9.58E-03	1.37E-02	0.00E+00	1.65E-03
ULI Wall	0.00E+00	4.16E-03	1.04E-02	1.45E-02	0.00E+00	7.27E-05
Heart Wall	0.00E+00	6.39E-02	2.36E-02	8.74E-02	5.25E-03	0.00E+00
Kidneys	0.00E+00	1.22E-02	1.11E-02	2.33E-02	1.40E-03	1.16E-04
Liver	0.00E+00	1.29E-02	1.40E-02	2.70E-02	1.62E-03	1.35E-03
Lungs	0.00E+00	1.37E-02	1.09E-02	2.46E-02	2.95E-03	2.95E-03
Muscle	0.00E+00	4.16E-03	7.97E-03	1.21E-02	0.00E+00	6.07E-05
Ovaries	0.00E+00	4.16E-03	1.28E-02	1.70E-02	4.25E-03	3.40E-03
Pancreas	0.00E+00	4.16E-03	1.12E-02	1.54E-02	0.00E+00	7.68E-05
Red Marrow	0.00E+00	2.84E-03	9.16E-03	1.20E-02	1.44E-03	1.44E-03
Osteogenic Cells	0.00E+00	9.58E-03	9.36E-03	1.89E-02	5.68E-04	1.89E-04
Skin	0.00E+00	4.16E-03	4.99E-03	9.16E-03	0.00E+00	9.16E-05
Spleen	0.00E+00	4.16E-03	8.97E-03	1.31E-02	0.00E+00	6.56E-05
Thymus	0.00E+00	4.16E-03	9.69E-03	1.39E-02	0.00E+00	6.93E-05
Thyroid	0.00E+00	4.16E-03	6.63E-03	1.08E-02	3.24E-04	5.40E-04
Urinary Bladder Wall	0.00E+00	1.17E-01	6.47E-02	1.82E-01	1.09E-02	9.11E-03
Uterus	0.00E+00	4.16E-03	1.73E-02	2.14E-02	0.00E+00	1.07E-04
Total Body	0.00E+00	5.59E-03	8.44E-03	1.40E-02	0.00E+00	0.00E+00

PET effective dose per unit activity (mSv/MBq) was calculated as 2.42E-02 for female patients administered ^{18}F-FDG radiopharmaceutical by OLINDA software.

Table 3.5 : Male patient results for ^{68}Ga-PSMA on excel page.

Target Organ	Alpha	Beta	Photon	Total	EDE Cont.	ED Cont.
Adrenals	0.00E000	2.42E-03	6.06E-03	8.48E-03	5.09E-04	2.12E-05
Brain	0.00E000	2.42E-03	1.10E-03	3.52E-03	0.00E000	8.80E-06
Breasts	0.00E000	2.42E-03	1.28E-03	3.71E-03	5.56E-04	1.85E-04
Gallbladder Wall	0.00E000	2.42E-03	5.50E-03	7.92E-03	0.00E000	0.00E000
LLI Wall	0.00E000	2.42E-03	2.97E-03	5.39E-03	0.00E000	6.47E-04
Small Intestine	0.00E000	2.42E-03	3.34E-03	5.76E-03	0.00E000	1.44E-05
Stomach Wall	0.00E000	2.42E-03	3.19E-03	5.62E-03	0.00E000	6.74E-04
ULI Wall	0.00E000	2.42E-03	3.32E-03	5.74E-03	0.00E000	1.43E-05
Heart Wall	0.00E000	2.42E-03	2.48E-03	4.90E-03	0.00E000	0.00E000
Kidneys	0.00E000	2.48E-01	2.63E-02	2.74E-01	1.64E-02	6.85E-03
Liver	0.00E000	2.46E-02	7.43E-03	3.20E-02	1.92E-03	1.60E-03
Lungs	0.00E000	2.42E-03	2.13E-03	4.55E-03	5.46E-04	5.46E-04
Muscle	0.00E000	2.42E-03	2.15E-03	4.58E-03	0.00E000	1.14E-05
Ovaries	0.00E000	2.42E-03	3.12E-03	5.54E-03	1.38E-03	1.11E-03
Pancreas	0.00E000	2.42E-03	5.18E-03	7.60E-03	0.00E000	1.90E-05
Red Marrow	0.00E000	1.03E-02	3.06E-03	1.33E-02	1.60E-03	1.60E-03
Osteogenic Cells	0.00E000	9.16E-03	2.31E-03	1.15E-02	3.44E-04	1.15E-04
Skin	0.00E000	2.42E-03	1.25E-03	3.67E-03	0.00E000	3.67E-05
Spleen	0.00E000	2.73E-02	7.22E-03	3.45E-02	2.07E-03	8.63E-05
Testes	0.00E000	2.42E-03	1.84E-03	4.26E-03	0.00E000	0.00E000
Thymus	0.00E000	2.42E-03	1.63E-03	4.06E-03	0.00E000	1.01E-05
Thyroid	0.00E000	2.42E-03	1.41E-03	3.83E-03	1.15E-04	1.92E-04
Urinary Bladder Wall	0.00E000	7.32E-02	1.11E-02	8.43E-02	5.06E-03	4.22E-03
Uterus	0.00E000	2.42E-03	4.14E-03	6.56E-03	0.00E000	1.64E-05
Total Body	0.00E000	4.49E-03	2.35E-03	6.85E-03	0.00E000	0.00E000

PET effective dose per unit activity (mSv/MBq) was calculated as 1.80E-02 for male patients administered ^{68}Ga-PSMA radiopharmaceutical by OLINDA software.

3.2 Effective Dose from CT

The calculation of computed tomography (CT) doses involves several methods, and the choice of method may depend on the specific parameters and data available. There are specialized software tools designed for CT dose estimation, such as ImPACT (Imaging Performance Assessment of CT Scanners). This tool employs mathematical models and phantom measurements to estimate organ and effective doses.

3.2.1 ImPACT CT dose calculator

ImPACT (Imaging Performance Assessment of CT Scanners) is a nonprofit organization based in the United Kingdom that specializes in providing information and resources related to radiation dose and image quality in medical imaging, particularly CT scanning. ImPACT is known for developing dose calculation tools and software for CT scanners. The software is designed to evaluate various aspects of CT imaging, including dose calculations, image quality, and other performance parameters. Figure 3.13 shows the phantom used for ImPACT.

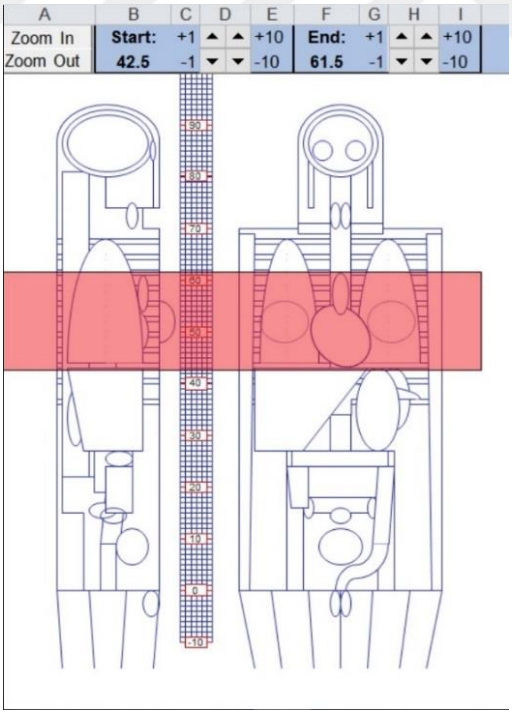

Figure 3.13 ImPACT software phantom (URL-7).

The ImPACT CT Dose Calculator is a specific tool developed to estimate the radiation dose associated with a CT imaging device. This tool takes into account various parameters, including the type of CT examination, scanning protocols, and patient

characteristics, to calculate an estimated dose. Figure 3.14 shows the interface of ImPACT software where input data is registered and also provide total effective dose.

Users typically input information such as the specific CT protocol being used, patient age and size, and other relevant factors. The calculator then provides estimation of effective dose and organ doses resulting from the CT examination. This information can be valuable for healthcare providers in ensuring that radiation dose is within ALARA exposure limits while still acquiring the necessary diagnostic information (URL-9).

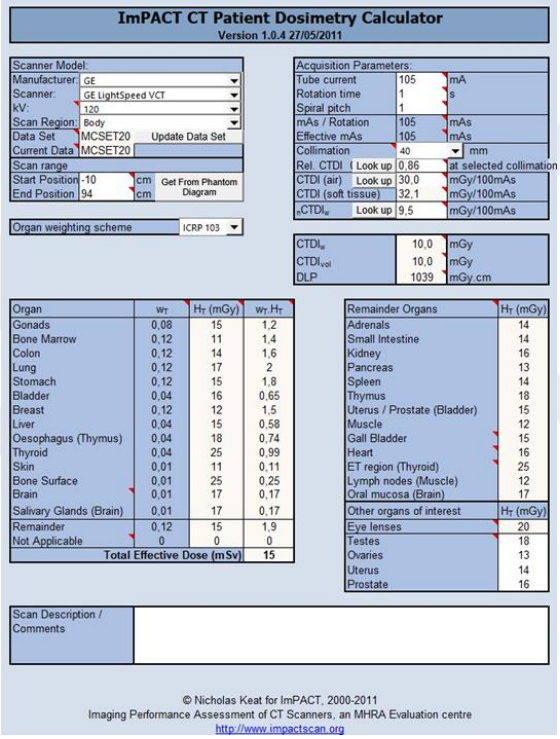

Figure 3.13 : ImPACT software interface. (Figure 3.14)

CT dose index (CTDI) is a standard measure for the output of radiation dose of a CT scanner, this measure ables the user to compare the radiation output of CT scanners that are not similar. $CTDI_{100}$ gets measured on an ionizing chamber that is 100 mm long and $CTDI_w$ gets weighted average of the dose through one slice; for the helical scanners that are being utilized currently the parameter CTDIvol will be the index that is used more commonly and it represents the average of the dose that is in the center central area of a multiple scan examination. The topographical variation of the body of a human being is not taken into consideration by $CTDI_{100}$ (mGy) so it is not in clinical use. $CTDI_w$ (mGy) is closer to the human dose profile as compared with the $CTDI_{100}$ and it is calculated by the following equation:

$$CTDI_W = \frac{1}{3} CTDI_{100}(center) + \frac{2}{3} CTDI_{100}(periphery) \quad (3.7)$$

CTDIvol (mGy) is obtained by dividing $CTDI_w$ by pitch factor:

$$CTDIvol = CTDI_w / pitch \quad (3.8)$$

Pitch means the table index per rotation divided by total nominal scan width (Jallow et al., 2016).

3.3 ICRP 60 and ICRP 103 Publications

ICRP Publication 60 described the recommendations from the ICRP, an independent organization offering guidance on radiation protection standards. Publication 60 replaced the previous recommendations (ICRP Publication 26) and established new guidelines for radiation protection (ICRP, 1991).

Key points from ICRP Publication 60 include the concept of dose limits for radiation exposure was introduced and also, the effective dose, considering the differing sensitivity of various tissues to radiation, was defined. Clear definitions of various radiation quantities and units were provided, helping to standardize terminology in the field. Guidelines for occupational exposure were outlined, taking into consideration the type of work and potential exposure scenarios. Special considerations for medical exposure were addressed, recognizing the benefits of diagnostic and therapeutic applications of radiation while emphasizing the need for optimization.

ICRP Publication 103 builds upon the foundation laid by Publication 60. It reflects advances in scientific understanding and technology in the years following the earlier publication (ICRP, 2007). Key features of ICRP 103 include the introduction of the concept of “dose constraint” to complement dose limits and emphasis on the role of justification, optimization, and the application of dose limits and constraints. ICRP 103 contained reaffirmation of the fundamental principles of radiation protection, including justification, optimization, and limitation. Also It includes updates on the understanding of biological effects, particularly in terms of tissue and organ doses besides revision of dose limits and the introduction of dose limitations for anticipated radiation exposures. Other key feature is further refinement of recommendations for occupational exposure, including considerations for emergency workers and pregnant workers.

Both ICRP 60 and ICRP 103 are critical documents in the context of radiation protection, providing a framework for establishing standards and practices to make sure the safe use of ionizing radiation. Tissue (or organ) weighting factors (w_T) are crucial parameters in calculating the effective dose for radiological protection. As stated before, they signify the varying sensitivity of different tissues and organs to stochastic effects induced by ionizing radiation, such as cancer.

3.3.1 Tissue weighting factors for ICRP 60 and ICRP 103

The tissue (or organ) weighting factors in ICRP Publication 103 were adjusted compared to Publication 60. The changes were aimed at reflecting updated scientific understanding and recommendations. The effective dose in ICRP 103 is calculated by adding up the product of the equivalent dose to each tissue or organ and its corresponding tissue weighting factor (w_T). The key modifications in tissue weighting factors from ICRP Publication 60 to 103 include adjustments for gonads and breast. The adjustments aim to better reflect the relative radiosensitivity of these tissues and organs. The overall structure of calculating the effective dose remains the same, with the sum of the products of equivalent doses and tissue weighting factors. Table 3.6 displays weighting factors according to ICRP 60 and ICRP 103. These factors help us understand how much each part of the body is affected by radiation (ICRP 60, 1991; ICRP 103, 2007).

Table 3.6 : Organ weighting factors for ICRP 60 and ICRP 103 (URL-6).

	w_T	
Organ	**ICRP 60**	**ICRP 103**
Gonads	0.2	0.08
Bone marrow (red)	0.12	0.12
Colon	0.12	0.12
Lung	0.12	0.12
Stomach	0.12	0.12
Bladder	0.05	0.04
Breast	0.05	0.12
Liver	0.05	0.04
Oesophagus	0.05	0.04
Thyroid	0.05	0.04
Skin	0.01	0.01
Bone surface	0.01	0.01
Brain	-	0.01
Salivary Glands	-	0.01
Remainder	0.05	0.12

4. RESULTS AND DISCUSSION

A 1-month retrospective study of PET/CT exams of the patients at the Nuclear Medicine department of Yeditepe University Kosuyolu Hospital were recorded during the period of January 2023. The study included 305 adult cases and the details for every and each patient were recorded to show the demographic informations (age and gender).

The study analyzed routine whole-body PET/CT scans from the hospital that met quality control standards, and the research adhered to the principles of the Declaration of Helsinki. Whole body PET/CT protocol from top of the head to the mid-thighs has been performed.

The type and specification of the device used at Nuclear Medicine department was General Electric Discovery 64 Slide 710. To calculate the effective dose, the scan parameters (administered ^{18}F-FDG and ^{68}Ga-PSMA activity, $CTDI_{vol}$) were used. The recorded parameters were documented on a separate data sheet. Tissue dose estimation in PET/CT examinations was performed using ImPACT, OLINDA/EXM and IDAC softwares. IDAC software allows for the calculation of the effective dose according to ICRP 60 and ICRP 103 tissue weighting factors whereas OLINDA/EXM calculate by ICRP 60 tissue weighting factor only. IDAC software enables to obtain the effective dose based on both old and new phantom whereas OLINDA/EXM software uses only old phantom described in ICRP 23 guideline.

Effective dose derived from CT imaging is calculated via ImPACT software and effective dose derived from PET Imaging is calculated via OLINDA/EXM and IDAC. Also, a MS-Excel application is used to record and to collect the data resulting from these software programs. PET organ doses are determined based on the radiopharmaceuticals injected, while CT tissue or organ equivalent doses are determined using a dosimetric parameters specific to the scanner.

Statistical analysis included mean, standard deviation, minimum, maximum and range.

4.1 CT Effective Dose

CT effective dose for each patient was calculated by using ImPACT interfaces given in section 3.2.1. Table 4.1 shows the CTDIvol and DLP from patient records for ^{18}F-FDG and ^{68}Ga-PSMA data. CT equivalent organ doses calculated by ImPACT for ^{18}F-FDG and ^{68}Ga-PSMA protocols were given in Table 4.2.

Table 4.1 : CTDIvol and DLP from patient records.

	CT Scan in ^{18}F-FDG Protocol		***CT Scan in ^{68}Ga-PSMA Protocol***	
	CTDIvol (mGy)	*DLP (mGy-cm)*	*CTDIvol (mGy)*	*DLP (mGy-cm)*
mean	12.66	1438.19	13.41	1502.57
SD	3.92	485.85	3.9	463.45
min	6.19	631.97	6.43	656.47
max	26.62	3357.66	26.55	3021.55

Table 4.2 : CT Organ doses.

Organs	**CT Equivalent Organ Doses (mSv)**	
	^{18}F-FDG Protocol	**^{68}Ga-PSMA Protocol**
Gonads	1.56±0.48	1.65±0.27
Bone marrow (red)	1.74±0.54	1.84±0.30
Colon	2.09±0.65	2.21±0.36
Lung	2.51±0.78	2.66±0.43
Stomach	2.32±0.72	2.45±0.40
Bladder	0.82±0.25	0.87±0.14
Breast	1.86±0.57	1.97±0.32
Liver	0.73±0.23	0.78±0.13
Oesophagus	0.94±0.29	0.99±0.16
Thyroid	1.25±0.39	1.33±0.22
Skin	0.14±0.04	0.15±0.02
Bone surface	0.32±0.10	0.34±0.06
Brain	0.21±0.07	0.23±0.04
Salivary Glands	0.21±0.07	0.23±0.04
Remainder	2.35±0.73	2.49±0.40
Effective Dose (mSv)	**19.05±5.89**	**20.17±5.87**

4.2 Patient Effective Doses for ^{18}F-FDG PET/CT

Table 4.3 shows patient nonclinical (weight and height) data and injected activities for the ^{18}F-FDG procedure. The mean±SD (range) ^{18}F-FDG injected activity was 458.06±48.84 MBq (203.5 to 584.6 MBq).

Table 4.3 : Patient nonclinical data and injected activity for ^{18}F-FDG.

	Weight (kg)	*Height (cm)*	*Injected Activity (MBq)*
mean	73.05	165.67	458.06
SD	14.07	9.11	48.84
min	39	145	203.5
max	120	190	584.6

Two softwares IDAC and OLINDA, based on ICRP 60 and ICRP 103 guidelines have been used for the PET dose calculation. Biokinetic data of ^{18}F-FDG has been introduced to the softwares for the effective dose estimation. Software interfaces of the biokinetic data and the organ absorbed doses per unit injected activity were given in section 3.1.3 for IDAC and OLINDA.

Table 4.4 shows effective doses from ^{18}F-FDG PET/CT scans. The mean ± SD (range) effective dose from the CT portion of scans was 19.05 ± 5.88 mSv (9.31 to 40.05 mSv). The PET doses from highest to lowest were calculated with OLINDA (old phantom, ICRP 60), IDAC (old phantom, ICRP 60), IDAC (new phantom, ICRP 60) and IDAC (new phantom, ICRP 103) respectively. Figure 4.1 shows mean effective doses and standard deviation for ^{18}F-FDG separating ICRP 60 and ICRP 103 guidelines as well as OLINDA and IDAC software programs. It's a summary of our ^{18}F-FDG findings, comparing the radiation estimates from different computer programs and ICRP guidelines.

Table 4.4 : Patient effective doses for ^{18}F-FDG PET/CT.

	CT Effective Dose (mSv)	*PET Effective Dose (mSv)*			
		IDAC			OLINDA
		New Phantom (ICRP 103)	*New Phantom (ICRP 60)*	*Old Phantom (ICRP 60)*	*Old Phantom (ICRP 60)*
mean	19.05	6.28	7.01	9.07	9.96
SD	5.88	0.67	1.18	1.42	1.58
min	9.31	2.79	2.63	3.46	3.79
max	40.05	8.01	9.48	12.13	13.34

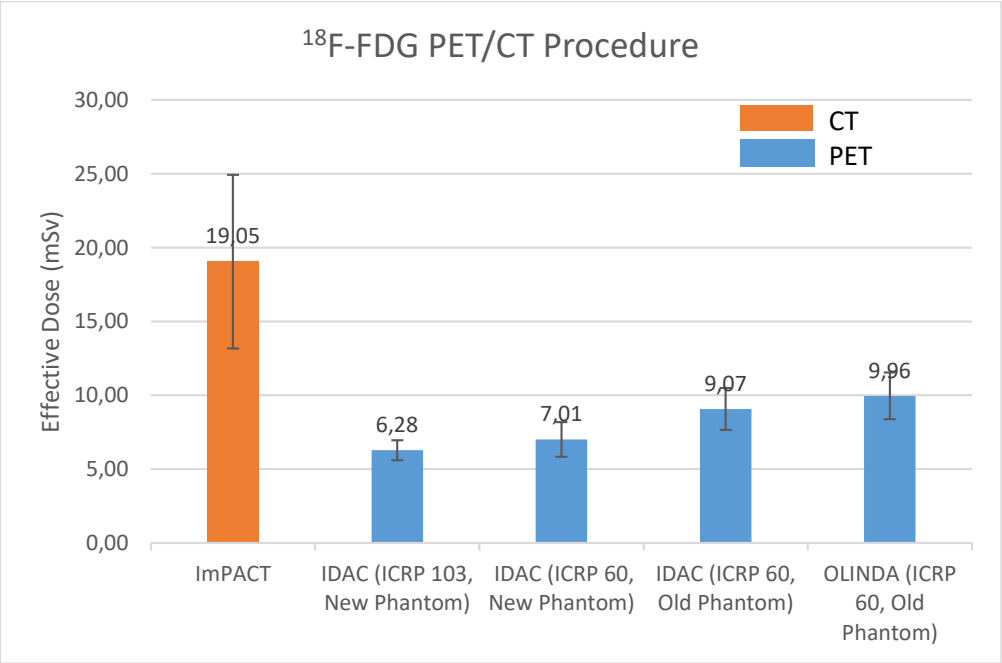

Figure 4.1 : Patient effective doses for ^{18}F-FDG PET/CT.

Depending on IDAC (new phantom), total effective dose for ^{18}F-FDG based on ICRP 60 and ICRP 103 is 26.06±3.53 mSv and 25.33±3.28 mSv, respectively. Total effective dose calculated with IDAC (old phantom) and OLINDA (old phantom) for ^{18}F-FDG based on ICRP 60 are 28.12±3.65 mSv and 29.01±3.73 mSv, respectively (Figure 4.1).

4.3 Patient Effective Doses for ^{68}Ga-PSMA PET/CT

Table 4.5 shows the ^{68}Ga-PSMA administered patient nonclinical data and injected activities. Mean administered activity for ^{68}Ga-PSMA is 202.02±29.6 MBq (136.9 to 310.8 MBq). ^{68}Ga-PSMA PET/CT effective dose was calculated with the same way we did for ^{18}F-FDG. ^{68}Ga-PSMA PET effective dose could not be calculated with the old phantom in IDAC software according to supplied biokinetic data.

Table 4.5 : Patient nonclinical data and injected activity for ^{68}Ga-PSMA.

	Weight(kg)	*Height(cm)*	*Injected Activity (MBq)*
mean	78.58	169.39	202.02
SD	13.70	10.85	29.6
min	50.00	105.00	136.9
max	140.00	183.00	310.8

Biokinetic data and organ absorbed doses per unit injected activity were given in section 3.1.3 for IDAC and OLINDA. Table 4.6 shows the effective dose calculated for ^{68}Ga-PSMA PET/CT.

Table 4.6 : Patient effective doses for ^{68}Ga-PSMA PET/CT.

		IDAC		OLINDA
		ICRP 103	*ICRP 60*	*ICRP 60*
	CT Effective Dose(mSv)	*PET Effective Dose(mSv)*	*PET Effective Dose(mSv)*	*PET Effective Dose(mSv)*
mean	20.17	1.83	2.07	3.65
SD	5.87	0.27	0.30	0.53
min	9.67	1.24	1.40	2.46
max	39.95	2.82	3.17	5.59

The mean ± SD (range) effective dose from the CT portion of scans was 20.17 ± 5.88 mSv (9.67 to 39.95 mSv). The PET doses from highest to lowest were calculated with OLINDA based on ICRP 60, IDAC based on ICRP 60 and ICRP 103 respectively. Figure 4.2 shows mean effective doses and standard deviation for ^{68}Ga-PSMA protocols separating ICRP 60 and 103 guidelines as well as OLINDA and IDAC software programs. It's a summary of our ^{68}Ga-PSMA findings, comparing the radiation estimates from different computer programs and ICRP guidelines.

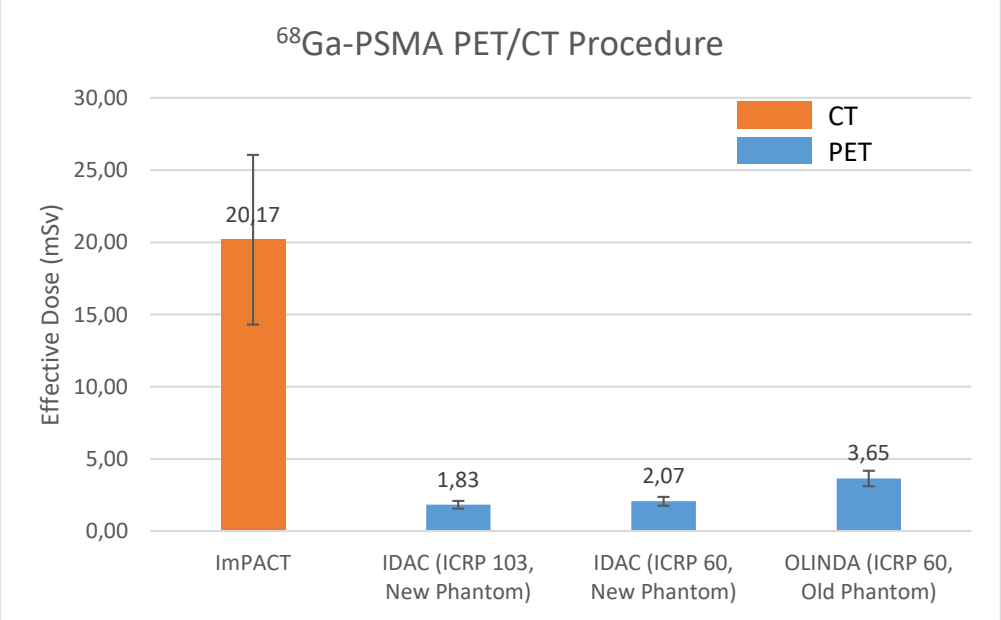

Figure 4.2 : Patient effective doses for ^{68}Ga-PSMA PET/CT.

Depending on IDAC results, total effective dose for ^{68}Ga-PSMA based on ICRP 60 and ICRP 103 is 22.24±3.09 mSv and 22.00±3.07 mSv, respectively. Total effective dose was calculated as 23.82±3.20 mSv with OLINDA based on ICRP 60 (Figure 4.2).

4.4 Comparing the Results

Statistical differences between groups of the data were evaluated using SPSS test and it was considered significant for $p<0.001$.

- IDAC PET effective dose calculated with ICRP 60 was significantly different from calculated with ICRP 103 tissue weighting factors ($p<0.001$). This difference shows that difference in tissue weighting factors lead to difference in effective dose estimated.
- IDAC and OLINDA softwares based on old phantom by ICRP 60 guideline calculates significantly different ($p<0.001$) effective doses. The effective dose calculations by IDAC and OLINDA vary even if effective dose calculated based on the same tissue weighting factors. It is because that OLINDA and IDAC may have different biokinetic models to simulate the behavior of radionuclides within the human body.
- IDAC old phantom and IDAC new phantom by ICRP 60 guideline effective dose results for each radiopharmaceutical are also significantly different ($p<0.001$). Variations in phantom geometry and composition can influence the dose calculations.

^{18}F-FDG PET effective dose percentage differences of IDAC (old and new phantom) and OLINDA softwares obtained with ICRP 103 and ICRP 60 guidelines can be seen in Table 4.7. PET ^{18}F-FDG effective doses by new phantom based on ICRP 60 guideline are about 11% higher compared to ICRP 103 guideline. It is because radioactivity is highly cumulated on bladders for FDG protocols and that cause high radiation exposure on its surroundings which is close to gonads. Tissue weighting factor for gonads has higher value in ICRP 60 and then, effective dose result was obtained higher compared to ICRP 103.

Table 4.7 : ^{18}F-FDG PET effective dose percentage differences.

		IDAC			OLINDA
		New Phantom		*Old Phantom*	*Old Phantom*
		ICRP 103	ICRP 60	ICRP 60	ICRP 60
IDAC New Phantom	ICRP 103	---	11%	36%	45%
	ICRP 60	11%	---	26%	35%
IDAC Old Phantom	ICRP 60	45%	26%	---	9%

The highest effective dose difference (45%) was obtained between IDAC (new phantom, ICRP 103) and OLINDA (old phantom, ICRP 60) due to the all parameters (phantom, biokinetic data and tissue weighting factors) are different. OLINDA (old phantom, ICRP 60) and IDAC (old phantom, ICRP 60) calculated relatively close effective doses (9%) as expected.

^{18}Ga-PSMA PET effective dose percent differences of IDAC and OLINDA softwares calculated with ICRP 103 and ICRP 60 can be seen in Table 4.8.

Table 4.8 : ^{18}Ga-PSMA PET effective dose percentage differences.

		IDAC		OLINDA
		ICRP 103	ICRP 60	ICRP 60
IDAC	ICRP 103	---	12%	66%
	ICRP 60	12%	---	55%
OLINDA	ICRP 60	66%	55%	---

Relatively close effective doses (9%) was obtained between IDAC results calculated with ICRP 103 and ICRP 60. However, the software difference caused a 55% difference in the effective dose. The highest effective dose difference (66%) was between OLINDA calculated with ICRP 60 and IDAC calculated with ICRP 103 tissue weighting factors. This is due to the use of different software as well as different tissue weighting factors.

Depending on IDAC results and ICRP 103 organ weighting factors, mean PET effective dose for whole body ^{18}F-FDG and ^{68}Ga-PSMA were 6.28±0.67 mSv and 1.83±0.27 mSv respectively. ^{18}F-FDG PET effective doses have been found to be greater than that of ^{68}Ga-PSMA PET doses. Mean administered activity for ^{18}F-FDG PET scan is 458.06±48.84 MBq, whereas this value is 202.02±29.6 MBq for ^{18}Ga-PSMA PET scan.

^{18}F-FDG PET effective dose results were compared with the literature in Table 4.9.

Table 4.9 : Comparison of ^{18}F-FDG effective dose results with literature.

Literature	Effective dose per administered activity mSv/MBq	PET ED (mSv)
Current study, 2024	0.013	6.28±0.67
Abuqbeitah et al., 2022	0.019	7.9
Anderrson et al., 2017	0.016	4.73
Climent et al., 2017	0.078	6.1±1.3
Quinn et al., 2016	0.020	9.0±1.6

CT scan is the main contributor to the total effective dose in the whole-body ^{68}Ga-PSMA and ^{18}F-FDG PET/CT protocols. For ^{68}Ga-PSMA protocol, CT contribution to the total effective dose was ~92%. Contribution of the CT effective dose to the total effective dose for ^{18}F-FDG protocol was ~75%. Table 4.10 shows the CT contribution to total effective dose by comparing with the previous studies for ^{18}F-FDG protocol.

Table 4.10 : Comparison of CT doses for ^{18}F-FDG protocol with previous studies.

Reference	E_{PET} (mSv)	E_{CT} (mSv)	E_{Total} (mSv)	CT dose contribution (%)
Current study, 2024	6.14	19.05	25.19	75.6
Sarah et al., 2020 (Saudi Arabia)	8	30	38	73
Paiva et al., 2019 (Brasil)	4.2	11.81	15	78.7
Kaushik et al., 2013 (India)	5.8	11.5	17.3	66.5
Khamwan et al., 2010 (Thailand)	4.4	14.45	18.9	76.5

5. CONCLUSION

In conclusion, this thesis has aimed to address the critical aspect of effective dose estimation for PET/CT procedures through the utilization of advanced computational tools, specifically IDAC (Internal Dose Assessment by Computer), OLINDA (Organ Level Internal Dose Assessment) and ImPACT (Imaging Performance Assessment of CT Scanners). The integration of these tools into the field of nuclear medicine dosimetry has provided valuable insights into the radiation exposure associated with PET/CT imaging.

Patient dosimetry for oncological PET/CT protocols with ^{18}F-FDG and ^{68}Ga-PSMA have been evaluated in Yeditepe University Koşuyolu Hospital. Clinical and non clinical data of total 305 patients were investigated and there is a difference in effective doses calculated with organ weighting factors by ICRP 60 and ICRP 103 besides phantoms and mathematicals models based on software programs. The study began with a comprehensive review of the principles underlying PET/CT procedures and the significance of accurate dose estimation for both diagnostic purposes and radiation protection. Subsequently, the application of IDAC and OLINDA in simulating the biokinetics of radiopharmaceuticals within the human body was explored. The use of computational phantoms and mathematical models confirmed instrumental in predicting organ and tissue doses.

The highlights of the study are given below:

- The results show that lower PET effective dose is calculated via updated software of IDAC including new phantom and ICRP 103 tissue weighting factors than the IDAC old version and OLINDA software.
- There are limited study related with ^{68}Ga-PSMA PET/CT patient doses. Only ^{18}F-FDG PET/CT patient doses could be compared with the literature. The reported administered activity for the different European countries ranged from 240 to 433 MBq (EC, 2015). In our country, the average injected activity was found to be 421 MBq in the largest ever study conveying analysis of 11-years

data of ^{18}F-FDG PET/CT scans (Abuqbeitah et al., 2022). The mean injected activity for ^{18}F-FDG (458 MBq) in this study is higher than the European countries. On the other hand, the Society of Nuclear Medicine and Molecular Imaging (SNMMI) Guidelines on Tumor Imaging with ^{18}F-FDG PET/CT suggests that adults are administered between 370 and 740 MBq (Delbeke et al., 2006).

- The effective dose for ^{18}F-FDG considering the organ weighting factors of ICRP 103 is 1.37 mSv/MBq, where the heart wall (0.052 mGy/MBq for male and 0.067 mGy/MBq for female) and urinary bladder wall (0.051 mGy/MBq for male and 0.054 mGy/MBq for female) receiving the highest organ dose per unit activity (Figure 3.5). Kidneys were the critical organ for ^{68}Ga-PSMA radiopharmaceutical and the highest absorbed dose per unit activity was found in kidneys (0.184 mGy/MBq for male and 0.218 mGy/MBq for female) (Figure 3.7).
- The five organs receving the highest organ equivalent doses from CT scans in order of highest to lowest dose were lung, stomach, colon, bone marrow (red) and gonads (Table 4.2). CT doses reported in the literature varied considerably, due to the wide variety of equipments and protocols (Rejeb and Sellem, 2023). For whole body FDG PET/CT procedures, the CT component contributing between 54 and 81% of the total combined dose depending on the CT parameters with the same scan length (Huang et al., 2009). Contribution of the CT effective dose to the total effective dose for ^{18}F-FDG protocols was ~75% in this sdudy.

As a coclusion, this study highlights that variations in radioactive decay data and discrepancies in phantoms contribute to differences in effective doses and the doses allocated to specific organs according to biokinetic data. The ICRP has included Adult Male/Female phantoms based on ICRP publications for assessing equivalent doses in organs regarding occupational, medical, or environmental radiation protection. These voxel models derive from medical image data averaged within a standard demographic. In reality, people are not always exactly like the average measurements used in medical procedures. This can lead to differences in the actual amount of radiation a person gets during medical tests. How much it varies depends on the specific physical characteristics of each person compared to the standard model.

Computer simulations to create specific phantoms for each patient requires an effort. Using this approach could make radiation dose measurements more precise and reliable but it is time consuming (Lacerda et al., 2020).

The calculated doses are generalized for a standard reference individual. For a more precise evaluation of radiation exposure from PET/CT procedures tailored to each and every patient, further information about individual biokinetics, anatomical specifics, and physiological characteristics is necessary.

REFERENCES

Abuqbeitah, M., Demir, M., Sönmezoğlu, K., Sayman, H., Kabasakal, L., Sağer, S., Asa, S., Beşli, L. U., Rehani, M. M. (2022). Patients undergoing multiple F-18 FDG PET/CT scans: frequency, clinical indications, and cumulative dose. *Health and Technology,* 13(1), 89-97. https://doi.org/10.1007/s12553-022-00716-0

Akpochafor, M., Omojola, A., Habeebu, M., Ezike, J., Adeneye, S., Ekpo, M., Aweda, M., Opadele, A., Orotoye, T. (2018). Computed Tomography Organ Dose Determination Using ImPACT Simulation Software: Our Findings in South-West Nigeria. *EJMO* 2(3), 165–172. DOI: 10.14744/ejmo.2017.75047;

Amis, S. E., Butler P. F., Appelgat, K. E., Birnbaum, S. B., Brateman, L. F., Hevezi, J. M., Mettler, F. A., Morin, R. L., Pentecost, M. J., Smith, G. G., Strauss, K. J., Zeman R. K. (2007). American College of Radiology White Paper on Radiation Dose in Medicine, *J Am Coll Radiol.* May;4(5):272-84.doi: 10.1016/j.jacr.2007.03.002.

Andersson, M., Johansson, L., Eckerman, K., Mattsson S. (2017). IDAC-Dose 2.1, an internal dosimetry program for diagnostic nuclear medicine based on the ICRP adult reference voxel phantoms. *EJNMMI Research*. 7:88. DOI 10.1186/s13550-017-0339-3

Andersson, M. (2015). Erratum to: effective dose to adult patients from 338 radiopharmaceuticals estimated using ICRP biokinetic data, ICRP/ICRU computational reference phantoms and ICRP 2007 tissue weighting factors. *EJNMMI Phys.* 2:22. DOI 10.1186/s40658-015-0121-4.

Attix F. H. (1986). Introduction to Radiological Physics and Radiation Dosimetry, WILEY-VCH Verlag GmbH & Co. KGaA, ISBN:9780471011460

Climent, J. M., Prieto, E., Morán, V., Sancho, L., Rodríguez-Fraile, M., Arbizu, J., García-Velloso, M. J., Richter, J. A. (2017). Effective dose estimation for oncological and neurological PET/CT procedures. *EJNMMI Research, 7:37,* DOI 10.1186/s13550-017-0272-5

Dash N. R., Dash A. (2011). Radiopharmaceuticals: A Review

Delbeke, D., Coleman, R. E., Guiberteau, M. J., Brown, M. L., Royal, H. D., Siegel, B. A. (2006). Procedure guideline for tumor imaging with 18F-FDG PET/CT 1.0. *J Nucl Med*. 47(5), 885–895.

Demirci, E., Toklu, T., Yeyin, N., Ocak, M., Alan Selcuk, N., Araman, A., Kabasakal, L. (2018). Estimation of the Organ Absorbed Doses and Effective Dose Form ^{68}Ga-PSMA -11 PET Scan. *Radiation Protection Dosimetry*. doi: 10.1093/rpd/ncy111

Ekpo, M., Obed, R. (2018). Patient Dose Estimation Using CT-Expo Software at Two Hospitals in North-Central Nigeria, *South. Clin. Ist. Euras.* 29(2), 125-131. DOI: 10.14744/scie.2018.78942

European Commission (EC) Medical Radiation Exposure of the European Population. Radiation Protection N° 180. 2015.

Günay, M., Özer, Y. PET Radiopharmaceuticals and Their Use in Hospital Practice in Turkey, International Conference on Integrated Medical Imaging in Cardiovascular Diseases (IMIC 2016)

Huang, B., Khong, P. (2009). Whole-body PET/CT scanning: estimation of radiation dose and cancer risk. *Radiology*, 251(1), 166-74. DOI: 10.1148/radiol.2511081300

International Atomic Energy Agency, Human Health Series, No. 26, Standard Operating Procedures for PET/CT: A Practical Approach for Use in Adult Oncology, IAEA, 2013.

International Commission on Radiological Protection ICRP 53, Radiation dose to patients from radiopharmaceuticals. Publication 53. Ann ICRP (1988)

International Commission on Radiological Protection ICRP 60, Recommendations of the International Commission on Radiological Protection. ICRP, Publication 60, (1991).

International Commission on Radiological Protection, ICRP 103, The 2007 Recommendations of the International Commission on Radiological Protection. ICRP Publication 103, (2007).

International Commission on Radiological Protection, ICRP 106, Publication Radiation Dose to Patient from Radiopharmaceuticals, (2007).

International Commission on Radiological Protection, ICRP 110, Realistic reference phantoms: An ICRP/ICRU joint effort. A report of adult reference computational phantoms, (2009).

International Commission on Radiological Protection, ICRP 23, Report on the Task Group on Reference Man, (1975).

Kamp A., Andersson, M., Leide-Svegborn, S., Noβke, D., Mattsson, S., Giussani, A. (2023). A revised compartmental model for biokinetics and dosimetry of 2-[18F] FDG. EJNMMI Physics, 10, https://doi.org/10.1186/s40658-023-00528-9

Kattan A. H., Numan, S. S. and Qutub, K. S. (2016). The History of Radiology: Achievements and Challenges

L'Annunziata M. (2020). The atomic nucleus, nuclear radiation, and the interaction of radiation with matter. Academic Press, https://doi.org/10.1016/B978-0-12-814397-1.00001-7.

Lacerda I., Vieira J., Oliveirad M., Lima F. (2020). Comparative analysis of the conversion coefficient for internal dosimetry using different phantoms. *Radiation Physics and Chemistry*, 167. https://doi.org/10.1016/j.radphyschem.2019.108351.

McCollough, C., S. Edyvean, B. Gould, N. Keat, P. Judy, W.Kalender, R. Morin, T. Payne, S. Stern, L. Rothenberg (2008). The Measurement, Reporting, and Management of Radiation Dose in CT cancer risk. *Radiology* 251 (1), 166–174.

Mettler, F. A., Guiberteau, M. J. (2018). Essentials of Nuclear Medicine and Molecular Imaging, ISBN: 9780323483193.

Murat, H., Karim, M. K. A., Kechik, M. M. A., Amer, M. F., Razak, H. R. A., Kamal, I., Chew, M. T. (2023). Internal dose assessment of lymphoma ^{18}F-FDG Positron Emission Tomography (PET) scan. *Journal of Physics: Conference Series*, doi:10.1088/1742-6596/2623/1/012003

National Council on Radiation Protection and Measurement, (2009). "Ionizing Radiation Exposure of the Population of the United States: NCRP REPORT No. 160

Paiva, F. G., Santana, P. C., Mourao, A. P., (2019). Evaluation of Patient Effective Dose in a PET/CT Test. *Applied Radiation and Isotopes*, 145, 137-141.

Powsner, R. A., Palmer, M. R., Powsner, E. R. (2013). Essentials of Nuclear Medicine Physics and Instrumentation, Wiley-Blackwell, ISBN: 978-1-118-47351-1

Quinn, B., Dauer, Z., Pandit-Taskar, N., Schoder, H., Dauer, L. T. (2016). Radiation Dosimetry of ^{18}F-FDG PET/CT: Incorporation Exam-Specific Parameters in Dose Estimates. *BMC Medical Imaging*, 16:41. DOI 10.1186/s12880-016-0143-y

Rejeb B. N., Sellem B. D. (2023). Evaluation of radiation doses of the ^{18}F-FDG PET/CT hybrid imaging in adult and paediatric oncologic patients. *Radiation Physics and Chemistry, 203.*

Stabin, M. G. (2007). Radiation Protection and Dosimetry, An Introduction to Health Physics, Springer.

Surti, S., Karp, J. S. (2016). Advances in time-of-flight PET. *Phys. Med.*, 32, 12–22.

Turner, J. E. (2007). Atoms, Radiation and Radiation Protection (Third Edit). Wiley.

Jallow N., Christian P., Sunderland J., Graham M., Hoffman j. M., Nye J. A. (2016). Diagnostic Reference Levels of CT Radiation Dose in Whole-Body PET/CT. The Journal of Nuclear Medicine., Vol 57.

UNSCEAR 2020/2021 Report, Sources, Effects and Risks of Ionizing radiation

URL-1 <https://www.researchgate.net/figure/Figure-13-The-photoelectric-effect-18_fig2_307466518

URL-2 <https://www.researchgate.net/figure/Schematic-representation-of-the-Compton-scattering_fig2_298709741

URL-3 <https://www.researchgate.net/figure/Figure-15-Pair-Production-18_fig4_307466518

URL-4 <https://www.researchgate.net/figure/First-medical-X-ray-by-Wilhelm-Roentgen-of-his-wife-Anna-Bertha-Ludwigs-hand-Wilhelm_fig1_339235859

URL-5 <https://www.mayoclinic.org/tests-procedures/pet-scan/multimedia/pet-plus-ct/img-20005900

URL-6 <https://www.researchgate.net/figure/ICRP-60-and-ICRP-103-weighting-factors_tbl1_47815241

URL-7 <https://www.researchgate.net/figure/Figure-1-Imagining-Performance-Assess-sment-of-Computed-Tomography-Scanners-ImPACT-The_fig1_3669 04059

WHO, 2023 https://www.who.int/news-room/questions-and-answers/item/radiation-and-health

CURRICULUM VITAE

Name Surname **:** Fatma Hilal BIKIRLI

EDUCATION :

- **B.Sc.** **:** 2017, Kocaeli University, Faculty of Technology, Department of Biomedical Engineering

PUBLICATION ON THE THESIS:

- **Bikirli, F. H.**, Altinsoy, N., Toklu, T, Effective Dose Estimation with IDAC for PET/CT Procedures, 2nd International Graduate Research Symposium-IGRS'23, 16-18 May 2023 (Online)